Contents lists available at ScienceDirect

Chemical Engineering Research and Design

journal homepage: www.elsevier.com/locate/cherd

SUSCAPE: A framework for the optimal design of SUStainable ChemicAl ProcEsses incorporating data envelopment analysis

Andres Gonzalez-Garay[a], *Gonzalo Guillen-Gosalbez*[a,b,*]

[a] *Department of Chemical Engineering, Centre for Process Systems Engineering, Imperial College, South Kensington Campus, London, SW7 2AZ, UK*

[b] *Departament d'Enginyeria Quimica, Universitat Rovira i Virgili, Av. Paisos Catalans 26, Tarragona, 43007, Spain*

ARTICLE INFO

Article history:
Received 5 October 2017
Received in revised form 21 May 2018
Accepted 6 July 2018
Available online 1 August 2018

Keywords:
Sustainable process design
Surrogate modeling
Life cycle assessment
Multi-objective optimization
Objective-reduction
Data envelopment analysis

ABSTRACT

Developing computer aided tools for process design is of paramount importance in the transition toward a more sustainable chemical industry. In this work, we present a framework to incorporate sustainability principles in the design of chemical processes that combines a palette of tools, including life cycle assessment, surrogate modeling, objective reduction, multi-objective optimization and data envelopment analysis (DEA). The latter methodology facilitates the post-optimal analysis of the Pareto front by narrowing down the number of designs and ranking them without the need to define weights in an explicit manner. DEA provides in turn improvement targets for the suboptimal alternatives that if attained would make them optimal, thereby guiding retrofit efforts toward the most effective actions based on benchmarking them against the best technologies available. The capabilities of the framework are demonstrated in a case study based on the production of methanol from CO_2 and hydrogen.

1. Introduction

Renewable and cleaner production systems are essential for ensuring a sustainable development. In the chemical industry, there is a growing trend to develop more sustainable processes based on the use of renewable materials, consumption of less energy and resources and generation of lower amounts of waste and emissions. As a result, new processes and technologies have emerged whose design and further implementation are now driven by sustainability criteria. The transition toward these new technologies will very likely take place in the coming decades, creating a clear need in the process industry to enhance current facilities so as to operate under more stringent sustainability criteria.

Given its natural link between fundamental science, engineering and industrial practice, the chemical industry plays a key role in meeting the challenges of sustainable development (Narodoslawsky, 2013). In particular, process design is at the core of sustainable development as it assists in the identification of process alternatives showing better economic and environmental performance. In this context, three main stages can be identified in the development of sustainable designs. The first stage is related to the modeling and assessment of the process under study. Here, sustainability metrics are selected and incorporated in the process model, which can be implemented following either equation-oriented or sequential modular approaches. In the second stage, the design task is posed as a multi-objective optimization (MOO) problem that seeks to minimize (or maximize) the sustainability metrics previously selected. Due to the existence of inherent trade-offs between them, these metrics tend to be in conflict with each other. Consequently, their optimization results in a set of optimal points that form the so called Pareto front of the problem. In the third stage, a post-optimal analysis is carried out to select the best design from the set of Pareto alternatives. This analysis is usually performed by stakeholders who are assisted by multi-criteria decision analysis (MCDA) tools.

* *Corresponding author.*
E-mail address: g.guillen05@imperial.ac.uk (G. Guillen-Gosalbez).
https://doi.org/10.1016/j.cherd.2018.07.009

Nomenclature

Abbreviations

AR	Assurance region
BCC	Banker-Charnes-Cooper DEA model
DEA	Data envelopment analysis
DMU	Decision-making unit
EA	Evolutionary algorithms
HEN	Heat exchanger network
LCA	Life cycle assessment
LCIA	Life cycle impact assessment
LP	Linear programming
MCDA	Multi-criteria decision analysis
MILP	Mixed-integer linear programming
MINLP	Mixed-integer nonlinear programming
MOO	Multi-objective optimization
NLP	Nonlinear programming
VRS	Variable returns to scale

Greek symbols

$\bar{\delta}$	Upper bound in approximation error $\delta_{s,s',i}$
$\delta_{p,p',i}$	Approximation error between solution s and s' in objective i
θ_o, θ	Technical efficiency of $DMU_{o/j}$
$\theta_{SE,j}$	Super-efficiency score of DMU j
λ_j	Linear weights of inefficient unit j to project it in the efficient frontier
μ_i	Relative error of the surrogate in objective f_i
φ	Non-Archimedean infinitesimal value

Variables

A	Matrix of multipliers preferences in dual model of DEA for outputs y_{ro}
ACC	Annual capital charge
B	Matrix of multipliers preferences in dual model of DEA for inputs x_{lo}
c	Number of decision-making units in DEA model
D	Matrix of multipliers preferences in dual model of DEA
f	Function to evaluate sustainability metric i
f_{imax}	Maximum value of objective f_i
f_{imin}	Minimum value of objective f_i
f_{ni}	Normalized value of f_i
$f_{p',i}$, $f_{p,i}$	Value of objective i in solution p'/p
FCOP	Fixed costs of operation
i	Number of objectives to optimize
j	DMU index
k	Objectives in the reduced space
K	Objectives in the full space
l	Index for inputs x in DEA model
m	Total number of inputs x in DEA model
n	Number of decision variables in design problem
P	Pareto set of design problem
p, p'	Pareto solution of set P
r	index for outputs y in DEA model
s	Total number of outputs y in DEA model
s_r^+	Output slack variable
s_l^-	Input slack variable
TAC	Total annualized cost
tol	Tolerance error for surrogate model in objective function f_i
u_r	Multiplier for output y_{ro}
v_l	Multiplier for input x_{lo}
VCOP	Variable costs of operation
w	Vector of decision variables in design problem
$\bar{X}$	DEA inputs expressing multipliers preferences in inputs x_{lo}
x_{lj}, x_{lo}	Input value of $DMU_{j/o}$ in input i
$\bar{Y}$	DEA outputs expressing multipliers preferences in outputs y_{ro}
y_{rj}, y_{ro}	Output value of $DMU_{j/o}$ in output r
$YP_{p,p',i}$	Binary parameter to denote dominance between solution s and s' in objective i
Z	Set of samples to evaluate in original model
$ZD_{p,p'}$	Binary variable to denote dominance between solution s and s' in the reduced space
ZO_i	Binary variable to denote if objective i is omitted
$ZOD_{p,p',i}$	Binary variable to denote if error $\delta_{s,s',i}$ is accounted

When assessing a chemical process and/or product, we must recall that sustainable development can only be achieved when considering the full environmental impact caused across all the stages in the product's life cycle. Among the different methods available to evaluate the environmental performance of products (Gong and You, 2017; Hui Liew et al., 2016; Khila et al., 2016; Ruiz-Mercado et al., 2016; Siew Ng and Martinez Hernandez, 2016), Life Cycle Assessment (LCA) ensures this holistic view by covering the extraction of raw materials and resources, production tasks, use, final disposal, waste management, and recycling stages (Azapagic, 1999; ISO, 2006). Because of such holistic approach and wide scope, LCA has become the prevalent methodology for environmental assessment, not only in the chemical industry but also in a wide range of areas in the private and public sectors (Jacquemin et al., 2012).

With regard to the process modeling, two main options emerge in process design. The first is to use equation-oriented approaches, which lead to non-convex mixed-integer nonlinear programming (MINLP) formulations that can be solved with state of the art software packages (e.g. GAMS, AIMMS, LINDO, MATLAB, etc.). This approach facilitates the optimization task, yet it typically relies on simpler and less accurate short-cut methods. These simplifications are required as otherwise the resulting MINLP can become too complex, making the optimization task challenging (Pattison et al., 2017; Steimel and Engell, 2016). This, of course, has an impact on the quality of the solutions found, which strongly depends on the model accuracy. Alternatively, the second approach refers to modular sequential models which rely on detailed equations of the unit operations and often generate more accurate results. While their formulation is still non-convex and nonlinear, they enable the use of tailored initialization techniques and solution algorithms that facilitate the convergence of the flowsheet (Caballero et al., 2005; Skiborowski et al., 2015). For these reasons, the sequential modular approach is widely used in many commercial simulators. Their downside, however, is that the algebraic expressions on which they are based are seldom explicitly available (e.g. Aspen-HYSYS, Pro II, etc.), thereby hampering the direct application of deterministic derivative-based optimization solvers.

Concerning optimization methods, the MINLPs arising in the equation-oriented approach are typically solved via standard deterministic optimization approaches. Here, the two most widely used algorithms are nonlinear branch and bound and outer approximation. When the models are multi-objective, they are first reformulated using an auxiliary single-objective formulation, which is then solved iteratively for a set of values of the auxiliary parameters (weights on objectives in the weighted-sum method and epsilon parameters in the epsilon-constraint algorithm). These methods cannot guarantee convergence to the global optimum due to the non-convexities in the MINLP. When the global optimum is sought, deterministic global optimization methods shall be applied, such as spatial branch and bound.

It should be noted that the computational resources of deterministic algorithms increases exponentially with the number of objectives. An additional consideration when using these algorithms concerns the need to devise a proper initialization scheme to identify feasible solutions for the algorithm from which to start the iterations. When the MINLP is modeled in a sequential modular approach using a commercial simulator, deterministic techniques cannot be applied in a direct manner anymore. This is because gradients are hard to obtain when the deterministic algorithms are coupled with the sequential simulator. In practice, gradients are often calculated by perturbing the simulation model in a given point, which creates numerical noise and convergence problems as iterations proceed.

Simulation-optimization approaches offer an appealing framework to decouple the modeling task from the optimization (Caballero et al., 2005; Ibrahim et al., 2017; Skiborowski et al., 2015). Following this approach, an optimization algorithm interrogates the simulator to get the value(s) of the objective function(s) and check that all the constraints are satisfied. After a set of iterations, a solution is finally reported when a termination criterion is met. In this context, derivative-free optimization algorithms are particularly appealing, as they are known to perform well in problems where discontinuous, non-differentiable, or highly nonlinear expressions are present. Although these algorithms cannot guarantee an "exact" optimal solution, their computational performance when dealing with large and complex systems usually outperform derivative-based algorithms without sacrificing much in terms of the accuracy of the final solution (Coello Coello et al., 2007). Among them, evolutionary algorithms (EA) are the most well-known techniques (Skiborowski et al., 2015). EA fall within the category of stochastic algorithms, which rely on a set of points to explore the design space. These methods require a function assigning a fitness value to every solution, also referred as individual. According to the evaluation of the fitness function, the algorithm modifies the initial set of individuals (population) using mutation and crossover operators and determines which individuals will survive in the next generation. Given that the "starting point" of the algorithm is the initial population, the quality of the solution generated depends on the initial individuals generated; nevertheless, the mutation and crossover functions attempt to improve the fitness of the individuals after each generation, making the algorithm less sensitive to the initial population. The application of EA algorithms in process design has increased over the last years, mainly due to their appealing properties when coupled with process simulators (Coello Coello et al., 2007; Ibrahim et al., 2017; Otte et al., 2016; Skiborowski et al., 2015; Valadi and Siarry, 2014). However, when complex processes are analyzed, care must be placed on several issues, including: the handling of constraints that cannot be included explicitly in the simulation; the selection of the decision variables and their boundaries; and the initialization of the entire flowsheet. Additionally, this approach can be hard to apply when the flowsheet requires a long time to converge or fails to do so for some values of the decision variables proposed by the optimization algorithm as iterations proceed (Ibrahim et al., 2017; Skiborowski et al., 2015).

An appealing alternative to overcome these limitations and further reduce the computational resources used during the optimization is to treat the flowsheet (or some of its unit operations) as a black-box using surrogate models to predict its performance (Biegler et al., 2014; Boukouvala et al., 2015; Caballero and Grossmann, 2008; Cozad et al., 2014). These surrogates, which are built from data generated with the original simulation, make the optimization task easier at the expense of sacrificing, to some extent, the accuracy of the model and quality of the final solution (Biegler et al., 2014; Boukouvala et al., 2015). The use of surrogates in simulation-based problems is a common practice (Boukouvala and Ierapetritou, 2013; Caballero and Grossmann, 2008; Cozad et al., 2014; Ye and You, 2016), yet their application in sustainability problems is still limited (Boukouvala et al., 2015; Cozad et al., 2014; Lin et al., 2017; Quirante et al., 2015a,b).

The sustainable process design problem is further complicated by the need to incorporate multiple sustainability criteria into the analysis (Guillén-Gosálbez et al., 2008), which leads to multi-objective problems whose complexity grows as the number of objectives increases. A natural trade-off arises at this point between an easier solution procedure and interpretation of results when omitting indicators, and more complex calculations and analysis when considering more sustainability criteria (Azapagic et al., 2016; Babi et al., 2015; Bertran et al., 2017; Gong and You, 2017; Grossmann and Guillen-Gosalbez, 2010; Hui Liew et al., 2016; Khila et al., 2016; Ruiz-Mercado et al., 2016; Serna et al., 2016; Siew Ng and Martinez Hernandez, 2016; Tula et al., 2017). One option to simplify the problem with minimum information loss relies on the use of objective-reduction techniques (Brockhoff and Zitzler, 2006; Brunet et al., 2012; Deb and Saxena, 2006; Guillén-Gosálbez, 2011). In the context of sustainability problems, these tools exploit the fact that in many LCA studies some indicators tend to correlate strongly with each other (Steinmann et al., 2016). In a seminal work, Brockhoff and Zitzler (2006) proposed an algorithm to obtain a reduced-order problem by eliminating objectives while preserving the characteristics of the Pareto frontier of the original problem. In their approach, redundant objectives are identified by quantifying a minimum approximation error. This algorithm was later modified by Guillén-Gosálbez (2011), who introduced a mixed-integer linear programming (MILP) model for dimensionality reduction based on the same concept of approximation error. This MILP provides the minimum combination of objectives that guarantees an approximation error below a given tolerance. This work has later been extended by other authors (Vázquez et al., 2018b, 2018a). Other works for dimensionality reduction in MOO rely on statistical tools, such as Principal Component Analysis, to omit objectives (Brunet et al., 2012; Deb and Saxena, 2006). While they usually lead to lower CPU times, they have the downside of not relying on any rigorous definition of approximation error. Because of this, they cannot ensure that the structure of the Pareto frontier is preserved after removing objectives.

The solution of a MOO is given by a Pareto frontier rather than by one single optimal solution, the latter being the case in single-objective problems. All the solutions contained in the Pareto frontier are optimal and have the property that one objective cannot be improved without worsening another one. In practice, the Pareto frontier is analyzed by stakeholders using multi-criteria decision analysis (MCDA) tools. Different MCDA approaches are available to select the best option among the Pareto points (Azapagic et al., 2016; Bortz et al., 2014; Huang et al., 2011; Miettinen and Hämäläinen, 1997), which often rank the alternatives on the basis of weights that reflect the decision-makers' preferences. The use of subjective weights represents the main limitation of these methods, which provide little insight on why some alternatives perform better than others. A different approach which overcomes this limitation is data envelopment analysis (DEA) (Lozano et al., 2008; Sueyoshi et al., 2017; Zhou et al., 2008a), a tool originally introduced in economics to assess different entities and that has recently received increasing interest in the assessment of sustainable systems. Based on the concept of efficiency, DEA classifies a set of units as efficient or inefficient, establishing targets for the improvement of the latter ones (Cook and Seiford, 2009). This is particularly appealing in process design, as improvement targets can guide retrofit efforts in sub-optimal technologies, classified as inefficient units, aiming for a more sustainable performance. Additionally, DEA allows filtering and ranking Pareto solutions, thereby facilitating the post-optimal analysis of the Pareto frontier. Some recent applications of DEA in sustainability-related topics cover energy and environmental efficiency (Korhonen and Luptacik, 2004; Sueyoshi et al., 2017; Vázquez-Rowe et al., 2015; Zhou et al., 2008b), energy policy-making (Li and Tao, 2017) and the assessment of flowsheets for fine chemicals (Mio et al., 2018), among many others (Galán-Martín et al., 2016).

In recent years, different approaches have been put forward to develop sustainable chemical processes (Azapagic et al., 2016; Babi et al., 2015; Bertran et al., 2017; Carvalho et al., 2014; Gong and You, 2017; Grossmann and Guillen-Gosalbez, 2010; Hui Liew et al., 2016; Khila et al., 2016; Nikolopoulou and Ierapetritou, 2012; Ruiz-Mercado et al., 2016; Serna et al., 2016; Siew Ng and Martinez Hernandez, 2016; Tula et al., 2017; Yue et al., 2013). Some of these approaches have focused on the development of appropriate indicators for the sustainability evaluation of products and processes (Carvalho et al., 2014; Dreyer et al., 2003; Khila et al., 2016; Sheldon, 2018). For instance, Carvalho et al. (2014) proposed a framework to select the most representative LCA indicators to be used in an environmental assessment according to the process being

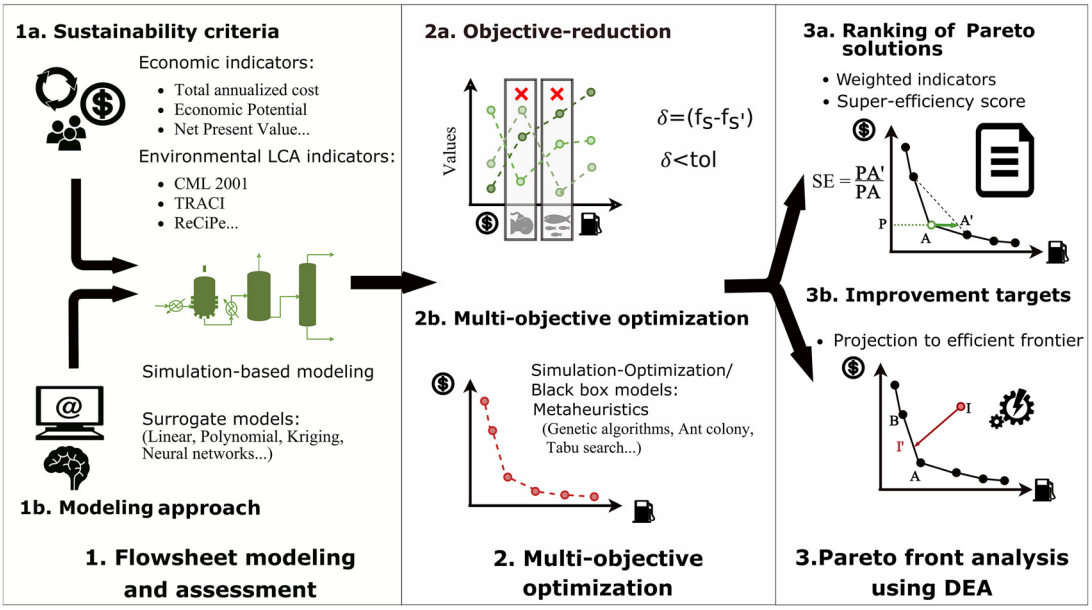

Fig. 1 – Framework for the optimal design of SUStainable ChemicAl ProcEsses (SUSCAPE).

modeled, while Khila et al. (2016) proposed a framework based on LCA indicators in conjunction with energy and exergy indicators. The vast majority of the approaches developed for the chemical industry couple environmental metrics with process modeling and/or optimization (Gong and You, 2017; Grossmann and Guillen-Gosalbez, 2010; Hui Liew et al., 2015; Khila et al., 2016; Ruiz-Mercado et al., 2016; Siew Ng and Martinez Hernandez, 2016). In this context, there is a general trend to develop process-based frameworks. However, as the chemical industry evolves, there is a clear need for more integrated systems shifting from process-based to macro-scale analysis (Gong and You, 2017; Wu et al., 2017; Yue et al., 2016). Examples of these types of frameworks are the works developed by Yue et al. (2016) and Gong and You (2017), where the process under study is not only analyzed as a unique entity but rather it is incorporated in a full network where its interactions with other processes is also accounted for in the analysis. More recently, Calvo-Serrano and Guillen-Gosalbez (2018) used as well network models of the petrochemical industry to assess the impact of some chemicals.

As we move to the application of macro-scale analysis, it will be necessary to improve the computational tools used for the modeling and optimization of chemical processes under sustainable indicators. Examples of the tools needed include the previously mentioned objective reduction algorithms (Brockhoff and Zitzler, 2006; Steinmann et al., 2016) and the use of simplified expressions based on rigorous thermodynamic models (surrogate models) (Boukouvala et al., 2015; Boukouvala and Floudas, 2016; Lin et al., 2017; Quirante et al., 2017; Ye and You, 2016). At both levels, different frameworks can be found that differ in the modeling approach and the solution procedure. Some works focus on single-objective optimization approaches that seek to improve the conceptual design of flowsheets by identifying "hotspots" and by replacing the units responsible for most of the impact. Examples of these frameworks are the works by Bertran et al. (2017), Babi et al. (2015) and Tula et al. (2017), where an initial superstructure defines potential candidates, which are further simulated using rigorous thermodynamic models. These models are then analyzed to identify improvement targets following process intensification principles. Other frameworks focus on multi-objective optimization, providing a Pareto frontier which has to be further analyzed to identify the most promising designs (Azapagic and Clift, 1999; Helmdach et al., 2017; Yue et al., 2016). In these methodologies, the analysis of the Pareto frontier is typically omitted. An exception is the work by Bortz et al. (2014), where the approach presented includes the modeling, multi-objective optimization and analysis of the Pareto frontier. From the different frameworks presented in the literature, we identified a clear need for approaches to accurately evaluate and optimize the sustainability performance of processes considering all their life cycle stages while requiring low computational resources.

In this work, we present a framework for the optimal design of sustainable chemical processes (SUSCAPE) that combines life cycle assessment, surrogate modeling, objective-reduction techniques, multi-objective optimization and multi-criteria decision analysis tools within a unified framework. The main novelty of SUSCAPE, additional to the integration of approaches, is the use of DEA to assess Pareto optimal designs. Hence, our approach goes beyond the calculation of the Pareto front, where most of the works in the literature end the analysis, to further screen and rank alternatives without the need of defining explicit weights on them. More precisely, and as discussed later in detail, in the context of process design DEA serves two main purposes: i) it filters and ranks Pareto solutions; and ii) it provides clear insight into how to make suboptimal solutions optimal through projections onto the efficient frontier.

The work introduced in this paper is organized as follows. In Section 2, we present in detail the methodology employed in SUSCAPE. In Section 3, the approach is applied to a case study based on the production of methanol from CO_2 and hydrogen. Finally, in Section 4 we present the conclusions and future work of the methodology.

2. SUSCAPE methodology

The methodology proposed for sustainable process design is outlined in Fig. 1. The first step in the framework is the definition of suitable metrics to quantify the economic and environmental pillars of sustainability. A process model is then implemented in a commercial simulator (e.g. Aspen-HYSYS, Aspen-Plus, SuperPro, etc.). When complex or computationally demanding processes are analyzed, surrogate models can be used to alleviate the computational effort during the optimization. Prior to the MOO stage, an objective reduction analysis is performed to omit redundant criteria. Herein, we use the MILP formulation introduced by Guillén-Gosálbez (2011). To solve the MOO problem, a multi-objective genetic algorithm (MOGA) is coupled with the process simulator (or surrogate model, when appropriate). The Pareto frontier generated during the optimization is finally analyzed using DEA to rank the Pareto optimal solutions and establish improvement targets for the suboptimal alternatives, which may often correspond to the business as usual designs.

It should be noted that here we focus mainly on process design rather than process synthesis. That is, we assume a fixed flowsheet structure for which we aim to determine the optimal equipment sizes, configurations and operating conditions. The optimization of superstructures could be carried out using the same approach, yet the computational requirements would grow. Each of the steps of our methodology is described in detail next.

2.1. Step 1: Flowsheet modeling and assessment

2.1.1. Sustainability assessment

While the framework is general enough to accommodate any metric, we focus here on economic and environmental criteria. Given that there is still a lack of general consensus on which social indicators could be included at the design stage, we decided to omit them from the framework. Nevertheless, these could be easily included at the time they become available. Economic indicators such as total annualized cost, economic potential or net present value can be easily incorporated into the model. As standard practice, we propose to use the total annualized cost (TAC), as it is widely applied in process design:

$$TAC = FCOP + VCOP + ACC \quad (1)$$

Where *FCOP* denotes the fixed costs of production, which include labor, maintenance, land, insurance, interest payments, overhead, license fees, and royalties; *VCOP* represents the variable costs of production, including raw materials, utilities, catalyst, and waste disposal; and *ACC* is the annual capital charge calculated using correlations available in the literature (Seider et al., 2009; Towler and Sinnott, 2013).

The environmental performance is assessed via LCA principles, as described by the International Organization for Standardization (ISO-14040) (ISO, 2006). The entries exchanged between the main process and the surroundings (technosphere) are obtained from the simulation model. These include raw materials, energy, steel required for the equipment construction, emissions, and waste generated. The inventory entries for the elements outside the boundaries of the plant can be retrieved from LCA databases (e.g. Ecoinvent, GaBi, ELCD, USDA, etc.). To translate the inventory data into impact categories, we can apply midpoint or endpoint life cycle impact assessment (LCIA) methodologies, such as TRACI, CML 2001, ReCiPe, etc. We recommend the use of midpoint indicators, as they avoid the application of subjective weights to aggregate the different environmental categories (Dreyer et al., 2003). Depending on the scope of the analysis, the process can be assessed from cradle-to-gate, cradle-to-grave or cradle-to-cradle.

As the boundaries to be modeled are expanded, the additional stages have to be properly defined and incorporated into the flowsheet of the process accordingly (distribution, final disposal, recycling, etc.). When the boundaries of the system are modified, the modeling shall be refined and the objective-reduction repeated to capture the new interactions between indicators. Furthermore, allocation of environmental burdens might be required for those processes producing by-products, using to this end mass or economic-based allocation procedures. In traditional techno-economic and environmental analysis, economic allocation analyzing the process from cradle-to-gate is the most common approach. However, the increasing level of integration within the chemical industry calls for more complex allocation methods and wider system boundaries based on sound LCA principles.

2.1.2. Process modeling

In SUSCAPE, we primarily focus on commercial simulators based on the sequential modular approach. These software packages calculate the outputs of each unit from the input streams and a set of design parameters. The advantages of using commercial simulators include the easy access to thermodynamic databases, the easy implementation of unit operations and modeling of flowsheets, and the robust initialization methods and tailored algorithms that facilitate the convergence of the model.

A fundamental part of process design and optimization is heat integration. In SUSCAPE, we retrieve the hot and cold streams from the simulator and externally calculate the composite curve, which provides the minimum theoretical utilities consumption. The targets for the hot and cold utilities obtained from the composite curve are then used to evaluate their cost and environmental impact. The detailed HEN design is therefore omitted, as it typically represents a small percentage of the total cost if a long enough period is chosen to annualize the capital cost (Smith, 2005). If desired, the framework could be easily adapted to incorporate the design of the HEN using MINLP formulations or similar approaches to generate more accurate results. However, the incorporation of such methods might increase the complexity of the model, thereby requiring larger computational resources.

The overall optimization is performed by decoupling the modeling step from the optimization task. In the modeling step, the system of nonlinear equations is solved in the simulator, while external functions calculate the composite curve and the values of the sustainability indicators. During the optimization, the solver seeks the best values for the design and operating variables by iteratively interrogating the simulator to obtain the objective function values and to check that the constraints are satisfied.

When complex or computationally expensive models are implemented in the simulator, the optimization task becomes challenging, as convergence problems, numerical difficulties, and/or large use of computational resources may arise (e.g. modeling reactive distillation columns, reactors with complex kinetics, several recycling streams, etc.) (Skiborowski et al., 2015). In such cases, surrogate models can be built to enhance the performance of the optimization solver.

Fig. 2 shows a general methodology for the generation of surrogate models. To clarify the methodology, let us first consider a number of objective functions f_i dependent on n design variables w_n. The approach starts by generating an initial set of samples Z_0 used to fit the surrogate. A traditional rule of thumb dictates that at least $10n$ samples should be generated within the upper and lower bounds of the design variables. These boundaries are typically established by a previous exploration of the model. In our framework, we apply the Latin Hypercube Design to generate the set of samples, as it shows good space-filling qualities (Mckay et al., 1979) (left-hand side box in Fig. 2). The simulator is then evaluated in the set Z_0 considering all the constraints of the process. As a result of the evaluation, feasible and infeasible samples will be identified (central box in Fig. 2). Feasible samples are used to calibrate the surrogate model, while infeasible and non-converged samples are discarded. Table 1 shows some of the most common forms of surrogates used in process design, all of which can be applied in the framework. At this stage, the boundaries of

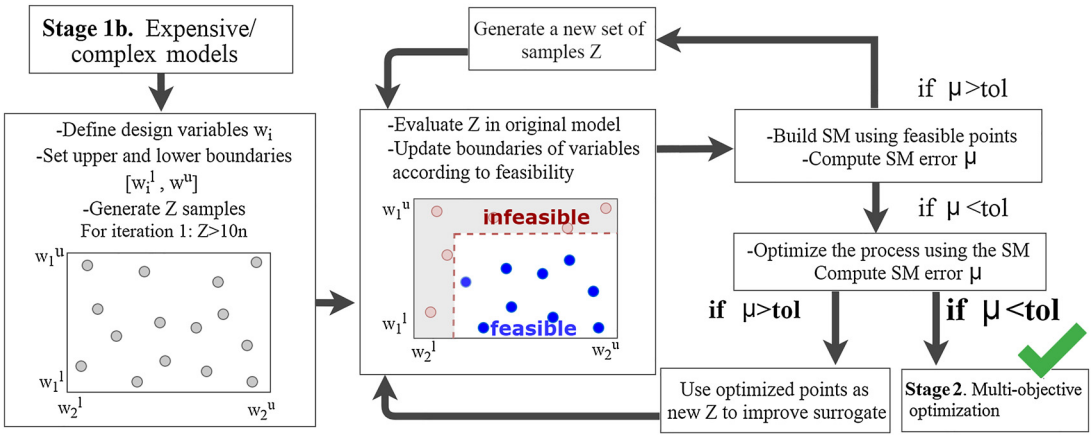

Fig. 2 – Surrogate models generation. [w_n denotes decision variables having upper w_n^u and lower w_n^l boundaries; f_i corresponds to the number of objectives to be optimized; Z represents the set of samples to be evaluated in the simulator; and μ represents the relative error measured for objectives f_i. The left hand side box represents the generation of samples within the decision variables space. In the central box, the samples are evaluated in the simulator, where the red dashed line defines the boundaries between the feasible and infeasible points.] (For interpretation of the references to colour in this figure legend, the reader is referred to the web version of this article.)

Table 1 – Standard modeling approaches used in process design for surrogate building.

	Model	
	Black box	Explicit algebraic models
Simulator (Ibrahim et al., 2017; Skiborowski et al., 2015)	x	x
Rigorous thermodynamic (Burger et al., 2014)		x
Surrogate models		
Linear (Boukouvala and Floudas, 2016)		x
Polynomial (Cozad et al., 2014)		x
Kriging (Boukouvala and Ierapetritou, 2013; Quirante et al., 2015a,b)		x
Neural networks (Nascimento et al., 2000)	x	x

the decision variables can be further adjusted to tighten the search space during the optimization (Boukouvala et al., 2015; Boukouvala and Floudas, 2016). After fitting the surrogate, a relative error μ_i is evaluated for all the objective functions f_i. If this error is below a given tolerance, the surrogate is considered to have enough accuracy and is used in the optimization; otherwise, the model has to be re-calibrated using more samples. If the accuracy sought cannot be achieved, a different surrogate form has to be selected. The complexity of the surrogate model is related to the accuracy required and the number of variables to optimize. In practice, a proper balance between computational performance and accuracy has to be found based on engineering knowledge of the problem.

Note that a different set of samples generated via the Latin hypercube design may lead to significantly different results (Boukouvala et al., 2015). Additionally, if the boundaries of the design variables are not well established, many of the sampled points might represent infeasible solutions (i.e. either because the constraints are violated or because the simulation model does not converge). The severity of this problem, which depends on the type of process analyzed, can be limited by increasing the number of samples. In some cases, the prediction error of the surrogate near the optimal solution might be large; that is, the optimal solution found by optimizing the surrogate will lead to simulation results that do not match well the surrogate output. In such cases, the samples generated in the optimization can be evaluated in the original model and then used to re-calibrate the surrogate. This can be done in an iterative manner until the error of the surrogate in the optimization falls ultimately below a given tolerance.

2.2. *Step 2: Multi-objective optimization*

2.2.1. *Objective reduction*

This stage is key, as the number of objectives significantly affects the performance of the optimization solver and the quality of the solutions obtained (Brockhoff and Zitzler, 2006). To perform the OR, we use the MILP formulation introduced by Guillén-Gosálbez (2011) and based on the approximation error presented by Brockhoff and Zitzler (2006). In Fig. 3, we outline the overall stages of the methodology and how it interacts with the MOO stage. After selecting the model to be used, an approximation of the Pareto frontier is first generated. This can be done by optimizing individually each objective separately or by optimizing pairs of them. The solutions obtained in these preliminary calculations are then normalized. In the next stage, some objectives are removed iteratively, and the dominance relationships between solutions are checked in the reduced space of indicators. An error is then calculated for each combination of objectives kept which takes into account how the dominance structure of the Pareto frontier changes compared to the full-space model. The algorithm ends when a maximum number of objectives has been removed while maintaining the error below a given tolerance. The full approach is explained in detailed in Appendix A.

2.2.2. *MOO optimization*

The sustainable design of chemical processes can be mathematically posed as an MOO problem of the following general form:

$$\min\left(f_1(w), f_2(w), \ldots, f_i(w)\right) \qquad \text{(P1)}$$
$$w \in W$$

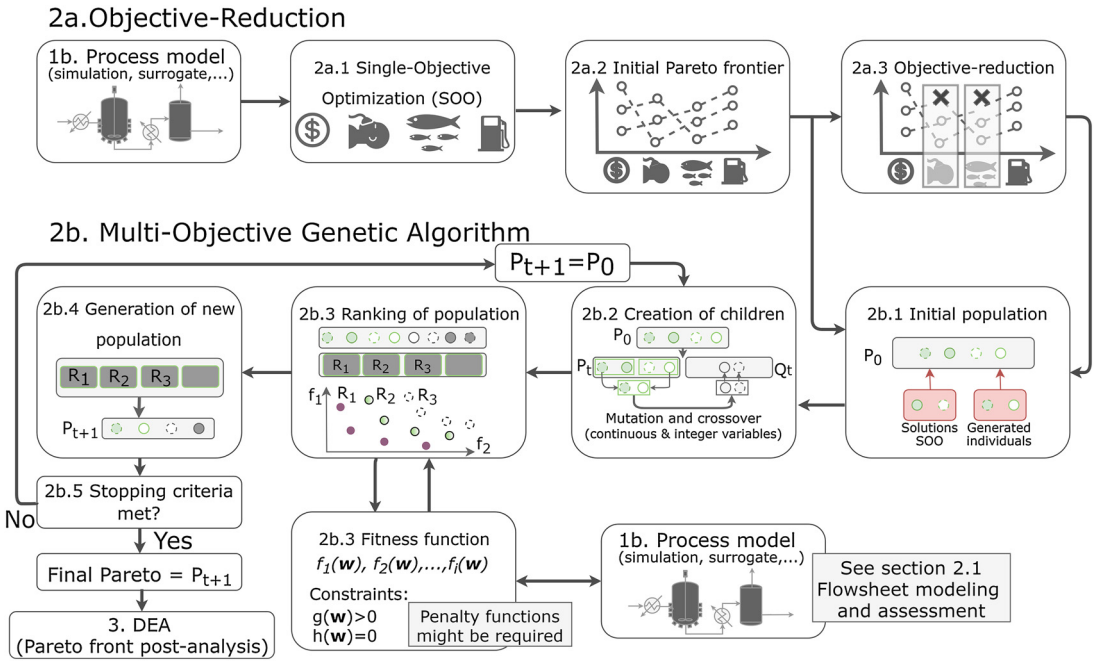

Fig. 3 – Flow of information between the objective-reduction, multi-objective genetic algorithm and process modeling.

Where there are $i \geq 2$ objectives and $\boldsymbol{w}$ is the vector of decision variables contained in the feasible region W, which is defined by equality and/or inequality constraints.

In SUSCAPE, without loss of generality, we focus on the use of Multi-Objective Genetic Algorithms (MOGA's) (Konak et al., 2006), as they can be easily coupled with simulators/black-box models and also with models based on algebraic expressions (Coello Coello et al., 2007; Ibrahim et al., 2017; Konak et al., 2006). MOGA's are particularly appealing as they handle simultaneously a set of points, also referred as individuals in a population, which allows them to find several members of the Pareto frontier in a single "run" of the algorithm. Likewise any evolutionary algorithm, the initial population in MOGA's is modified as iterations proceed according to the internal ranking of the population, which is generated by applying mutation and crossover functions (Coello Coello et al., 2007). To perform the optimization, the MOGA evaluates a fitness function for the given number of individuals in the population and iterates until a convergence criterion is met. The fitness function contains all the information required to evaluate the sustainability metrics. When coupling the MOGA with commercial simulators, the fitness function is computed by calling the simulator and retrieving the mass and energy balances, sizes of the equipment units, and hot and cold streams, which are all used to assess the sustainability metrics. When surrogate models are implemented, the fitness function is already given by the surrogate, which is constructed using the values of the fitness function for every sampled point. Penalties are employed to deal with the constraints that cannot be handled directly by the simulator or the surrogate (Ibrahim et al., 2017; Skiborowski et al., 2015). Fig. 3 shows the general optimization procedure and how it interacts with the modeling and objective-reduction stages.

2.3. *Pareto frontier post-analysis using data envelopment analysis (DEA)*

The solution of the MOO problem provides a set of Pareto points. In SUSCAPE, we analyze such solutions using data envelopment analysis. DEA is a linear programming (LP) technique that quantifies the relative efficiency of a group of comparable decision-making units (DMU's), each consuming multiple inputs to produce multiple outputs (Charnes et al., 1978). In our case, a DMU refers to one process design analyzed under multiple sustainability criteria such as total cost, global warming potential, human toxicity, etc. DEA provides efficiency scores for all the DMUs. Those with an efficiency of one are deemed efficient and ideally represent the best practices. The inefficient ones show an efficiency score strictly less than one, and for them improvement targets are defined such that, if attained, would make them optimal. DEA allows also to rank the efficient units by applying the super-efficiency concept. DEA is therefore used in our framework to: i) filter and rank the optimal solutions of the Pareto frontier; and ii) to determine improvement targets (in terms of sustainability performance) of a given process identified as inefficient.

DEA can be applied using either input or output oriented models (Cook and Seiford, 2009). Herein, we follow the input-oriented model, which aims to minimize the inputs (e.g. total annualized cost, global warming potential, etc.) while maintaining the same level of outputs (e.g. profit, amount of products and by-products produced, etc.). The technical efficiency of a DMU, θ_o ($o = 1, \ldots, c$), defined as the ratio of the weighted sum of s outputs y_{rj} ($r = 1, \ldots, s$) and the weighted sum of m inputs x_{ij} ($i = 1, \ldots, m$), is obtained by solving the BCC model (Banker–Charnes–Cooper) (Banker, 1984). This nonlinear model assumes variable returns to scale (VRS),

which implies that changes in outputs are not proportional to changes in inputs:

$$\max \theta_o = \frac{\sum_{r=1}^{s} u_r y_{ro} - u_o}{\sum_{l=1}^{m} v_l x_{lo}}$$
$$\sum_{r=1}^{s} u_r y_{rj} - u_o - \sum_{l=1}^{m} v_l x_{lj} \le 0; \quad j = 1, \ldots, n \qquad \text{(P2)}$$
$$u_r, v_l \ge 0; \quad \forall l, r; \quad \theta_o \text{unconstrained}$$

Where multipliers u_r and v_l denote weights given to inputs x_{lo} and outputs y_{ro}, respectively. In the model, these multipliers are optimized in order to maximize the efficiency value of DMU_o; hence, weights are optimized rather than given by decision-makers. From the solution of the model, those designs with an efficiency $\theta_o = 1$ are considered as efficient, while those with an efficiency $\theta_o < 1$ are considered as inefficient.

In DEA, it is also possible to define constraints on multipliers u_r and v_l according to the decision-makers' preferences. For instance, let us consider a process where we analyze the total annualized cost (TAC) and global warming potential (GWP) and in which GWP is given more importance than the TAC. This priority can be mathematically expressed via an algebraic constraint that forces multiplier v_{GWP} to be greater than multiplier v_{TAC} (we assume here that input and output data are both normalized). As a result, when attempting to make a DMU optimal, the model will not have the freedom to choose any arbitrary weights. Consequently, only those DMUs for which an efficiency of one can be obtained while fulfilling specific constraints on the weights will emerge as efficient, while the remaining DMUs will be deemed as inefficient.

The nonlinear model P2 can be reformulated into its equivalent linear program by setting to one the denominator of the efficiency in P2 (Banker, 1984):

$$\max \sum_{r=1}^{s} u_r y_{ro} - u_o$$
$$\sum_{l=1}^{m} v_l x_{lo} = 1$$
$$\sum_{r=1}^{s} u_r y_{rj} - u_o - \sum_{l=1}^{m} v_l x_{lj} \le 0; \quad j = 1, \ldots, n \qquad \text{(P3)}$$
$$u_r, v_l \ge 0; \quad \forall l, r; \quad \theta_o \text{unconstrained}$$

Similarly, model P3 can also be reformulated into a partner dual problem, which provides both, the efficiency scores and improvement targets for the inefficient units. The dual problem is expressed as follows (Banker, 1984):

$$\min \theta_o - \varphi\left(\sum_r s_r^+ + \sum_l s_l^-\right)$$
$$\sum_j \lambda_j x_{lj} + s_l^- = \theta_o x_{lo}; \quad l = 1, \ldots, m$$
$$\sum_j \lambda_j y_{rj} - s_r^+ = y_{ro}; \quad r = 1, \ldots, s \qquad \text{(P4)}$$
$$\sum_{j=1}^{n} \lambda_j = 1 \quad j = 1, \ldots, n$$
$$\lambda_j, s_l^-, s_r^+ \ge 0; \quad \forall i, j, r; \quad \theta_o \text{unconstrained}$$

Where φ is a non-Archimedean infinitesimal value used to enforce the variables to be strictly positive; s_r^+ is a slack variable representing the additional amount of output r required by DMU_o to become efficient; s_l^- is a slack variable denoting the amount of input l to be reduced to become efficient; and λ_j are the linear weights used to project the inefficient units onto the efficient frontier using a combination of efficient units. When $\theta_o = 1$ and $\left(s_i^- + s_r^+\right) = 0$, the DMU is said to be strongly efficient. If $\theta_o = 1$ but $\left(s_i^- + s_r^+\right) \neq 0$, the DMU is deemed as weakly efficient. If $\theta_o < 1$, the DMU is inefficient.

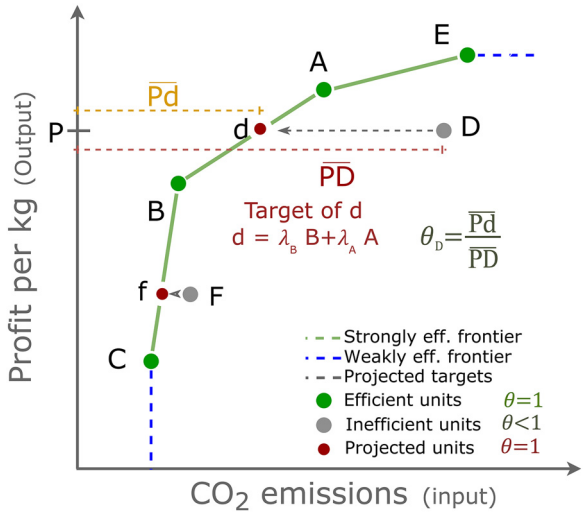

Fig. 4 – Graphical representation of DEA.

To further illustrate and clarify these concepts in the context of process design, let us consider technologies A–F that produce the same amount of a given chemical product. In the analysis, we aim to minimize the CO_2 emissions (modeled as an input), while maintaining the profit per kg of final product in each technology (modeled as an output). The graphical representation of the problem is shown in Fig. 4. We can identify technologies A, B, C, and E as efficient, meaning that they lie in the convex envelope of the Pareto front and there are no designs performing better than these alternatives simultaneously in both criteria. Technologies D and F are instead classified as inefficient ($\theta_o < 1$), as they are dominated by at least another design lying on the Pareto front. To become efficient, technologies D and F should be projected onto the efficient frontier. As the reader may have noticed, there is an infinite number of potential projections, being the input-oriented and output-oriented projections the most common approaches. Here, we focus on the input-oriented approach, in which to become efficient technologies D and F should reduce their level of CO_2 emissions until reaching the efficient frontier (points d and f, respectively). In contrast, the output-oriented model would require increasing the profit (output) for the same level of emissions (inputs).

Filtering of Pareto solutions. As shown in Fig. 4, the units identified as efficient by DEA are those lying on the convex envelope of the Pareto front. Units which are not part of this efficient frontier are inefficient. DEA can, therefore, be used to filter out the points generated by any MOO algorithm, ultimately retaining only the ones lying on the convex envelope of the efficient units. This is shown for the case of technology F in Fig. 4. Despite being Pareto optimal, it lies on the non-convex part of the Pareto front, so DEA would classify it as inefficient (with a θ_o value close to one). This filtering step helps to narrow down the number of optimal designs, thereby reducing the complexity of the post-analysis of the Pareto frontier. Additionally, as will be discussed later during the article, we can

further reduce the number of solutions kept by including a set of constraints reflecting priorities on sustainability metrics.

2.3.1. *Enhancement of technologies*

As shown in Fig. 4, the input-oriented DEA model determines the efficiency θ_o as the ratio between the level of inputs of a given unit and the level of inputs in the efficient frontier. This means that inefficient units (D and F) can be enhanced by projecting them on the efficient frontier (i.e. points d and f, respectively). The maximum reduction in inputs necessary for such DMUs to become efficient is given by the difference between the observed point and its projection onto the frontier. In DEA, the improvement target for input l in a given DMU is expressed as:

$$\sum_{j=1}^{n} \lambda_j x_{lj} = \theta_o x_{lo} - s_l^- \tag{2}$$

Coming back to the example shown in Fig. 4, technology D can become efficient by projecting it to point d, which implies that the same profit should be achieved while releasing less CO_2 emissions. For this case, the improvement targets for technology D are obtained using a linear combination of technologies A and B ($d = \lambda_B B + \lambda_A A$). In some cases, it might not be possible to practically achieve these targets, yet they allow identifying hotspots and sources of inefficiencies that can be employed to guide retrofit efforts toward more effective actions.

2.3.2. *Ranking of efficient (optimal) solutions*

DEA can also be applied to further rank the Pareto points of the model. This is achieved by using a super-efficiency model (Andersen and Petersen, 1993), which is essentially the same as the one described in P4, but in which the summation of lambdas excludes the efficient unit being assessed:

$$\sum_{j=1, j\neq j'}^{m} \lambda_j x_{lj} + s_l^- = \theta_j x_{lj'}; l = 1, \ldots, m \tag{3}$$

$$\sum_{j=1, j\neq j'}^{s} \lambda_j y_{rj} - s_r^+ = y_{rj'}; r = 1, \ldots, s \tag{4}$$

In an input-oriented model, the super-efficiency can be seen as the input savings achieved by an efficient DMU, which are measured by the extent to which the efficient frontier changes when such unit is removed. The modified DEA model therefore provides a super-efficiency score $\theta_{SE,j'}$ that is always greater or equal to one and can be used to further discriminate among efficient solutions. To exemplify this, let us consider the efficient technologies A, B, C, and E previously described and now shown in Fig. 5. If we analyze solution B, we can see that the amount of CO_2 emissions released can increase until point b without the unit becoming inefficient. This hypothetical increase can be considered as an input saving when compared to the remaining technologies. Note that this analysis fails when we consider design E, as there are no technologies releasing more CO_2 emissions while achieving the same level of profit. Given that this technology has the largest emissions of CO_2, we denote $\theta_{SE,E} = 1$, indicating a zero input saving for design E.

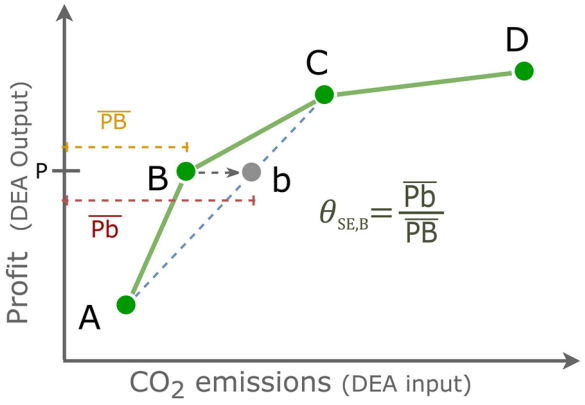

Fig. 5 – Graphical representation of the super-efficiency score.

3. Case study

To better illustrate the capabilities of SUSCAPE, we analyze the production of methanol from CO_2 and hydrogen, which has been identified as a promising route in carbon capture utilization (CCU) (Pérez-Fortes et al., 2016). The aim of the analysis is to optimize the process under sustainability criteria, obtaining a Pareto frontier which will be further analyzed using DEA. In order to show the different applications of SUSCAPE, we include in the analysis a base case taken from Pérez-Fortes et al. (2016).

Step 1: Flowsheet modeling and assessment. The flowsheet of the process is shown in Fig. 6, where CO_2 and hydrogen react to produce methanol and water. In a secondary reaction, the same reactants produce CO and water. CO_2 is obtained at 25 °C and 1 bar and is pressurized up to 78 bar through a series of four compressors. Hydrogen is available at 30 bar and needs to be pressurized up to 78 bar. Both gases are mixed and heated to carry out the reaction in a PFR modeled according to the kinetics reported by Vanden Bussche and Froment (1996). The process requires 44,500 kg of $Cu/ZnO/Al_2O_3$ catalyst.

The outlet of the reactor is cooled down and sent to a flash unit where part of the CO_2 and hydrogen mixed with CO are recovered and recycled back to the process. Some of the gases are released to avoid the accumulation of mass within the process. The pressure of the liquid stream coming out from the flash unit is lowered and the stream is then sent to a second flash where most of the remaining CO_2 and hydrogen are separated from water and methanol. Finally, the liquid stream of the second flash is heated prior to the distillation column, where methanol is recovered with a mass purity of at least 99.9 wt. %. The production rate of methanol is fixed to 440 kt/y, an average representative value used in conventional plants (Pérez-Fortes et al., 2016). The gas emissions of both flashes can be released to the environment or used to generate steam at high pressure, which requires the addition of a furnace in the flowsheet. The wastewater is sent to treatment. The decision variables to be optimized are shown in Table 2. Similarly, we also present in Table 2 the values for the base case (BC) taken from Pérez-Fortes et al. (2016).

Step 1a Sustainability assessment: The sustainability of the process is assessed from cradle-to-gate defining 1 kg of methanol as functional unit. The indicators considered were the TAC and those included in the LCIA methodology CML 2001: acidification potential (AP), global warming potential (GWP), depletion of abiotic resources (DAR), fresh aquatic ecotoxicity (FAET), marine aquatic ecotoxicity (MAET), terrestrial

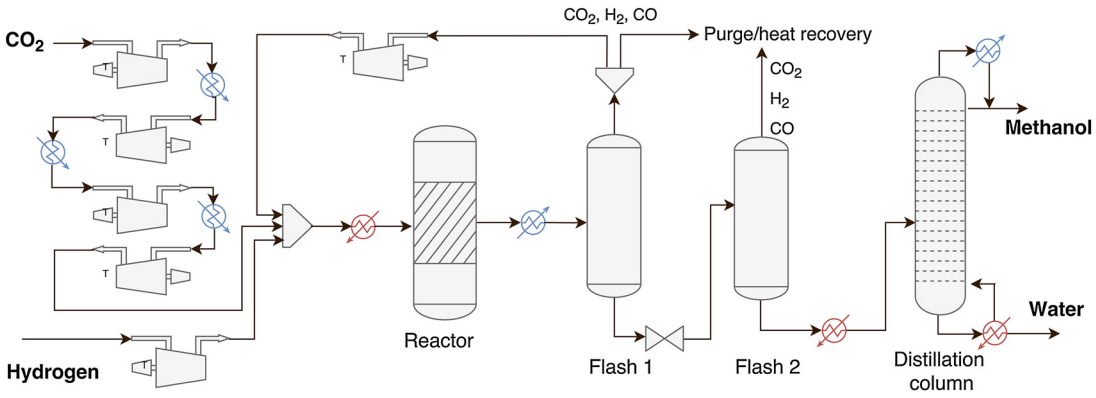

Fig. 6 – Methanol production process.

Table 2 – Decision variables in the methanol production process.

Variable	Flow rate CO_2 kmole/h	Flow rate H_2 kmole/h	T_{in} reactor °C	Reactor vol m^3	Recycling ratio	Heat recovery purge
BC	1830	5455	210	45	0.99	1
Lower bound	1500	4500	180	20	0.950	0
Upper bound	2300	6500	240	80	0.999	1

Variable	Pressure dist. kPa	T_{in} dist. °C	Reflux ratio	Methanol recovery	# of trays (Integer)	Feed tray (Integer)
BC	100	80	1.2	99.45	57	38
Lower bound	100	40	0.8	90.00	10	15
Upper bound	200	120	6.0	99.90	80	75

ecotoxicity (TE), eutrophication potential (EP), human toxicity (HT), ozone layer depletion (OLD) and photochemical oxidation (PO). Therefore, a total of 11 indicators were considered.

For the economic evaluation, costs were taken from Pérez-Fortes et al. (2016). Equipment costs were calculated using correlations reported in the literature (Seider et al., 2009; Towler and Sinnott, 2013). The environmental entries lying outside the boundaries of the plant were taken from the Ecoinvent database (Wernet et al., 2016) according to the processes described in Table 3. No allocation method is considered as methanol is the only product of the process.

For simplicity, we assume that the cost of the CO_2 captured is given by the electricity consumed during the compression stage. Note that the impact embodied in this electricity is already accounted for in the CO_2 production process available in Ecoinvent. In the GWP category, each kilogram of CO_2 in the feed stream was considered as a credit (–1 kg of CO_2-eq) and subtracted from the value reported in the database for the production of CO_2, resulting in a net value of −0.27 kg of CO_2-eq/kg of CO_2 consumed.

Step 1.2 Process modeling. The detailed process was first modeled in Aspen-HYSYS and then used to build a surrogate model constructed with neural networks. The decision variables considered and their boundaries during the sampling are shown in Table 2. During the sampling and further optimization, all the variables were allowed to vary according to the values in Table 2 and fixing the methanol purity to 99.9 wt. % in the simulation. The only additional constraint which was not imposed in the simulator was a minimum methanol production rate.

With regard to the surrogate model, it was built using neural networks given their high degree of accuracy (Himmelblau, 2008). The surrogates were developed for the entire flowsheet rather than for its individual components separately. A summary of the surrogate building and calibration is provided in Fig. 7, which shows how the convergence and feasibility of the sets improved as the model was re-calibrated and the boundaries of the variables tightened. The initial set of samples (set $Z_1 = 1000$) used to construct the surrogate was generated via the Latin hypercube design within the boundaries shown in Table 2. From the 1000 samples generated, 590 converged in the simulation, while 51% of these converged simulations (209 samples) achieved the production rate, which was the only external constraint considered in the analysis. To build the surrogate, 70% of the feasible samples were used to train the model, 15% to validate it and 15% to test it. In the validation stage, the parameters of the surrogate are still tuned after the training. During the test stage, the parameters of the surro-

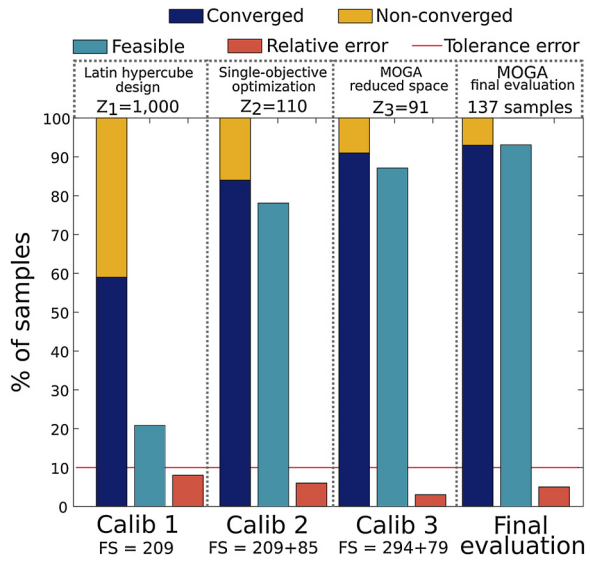

Fig. 7 – Summary of the surrogate evaluation. The surrogate was first built and then re-calibrated two times adding the feasible samples (FS) of each set. Initial iteration: 209/1000 samples, re-calibration one: (209 + 85)/(1000 + 110) samples; re-calibration two: (294 + 79)/(1110 + 91) samples.

Table 3 – Economic and environmental data for the methanol production process.

Commodities	Cost (€/unit)	Production process taken from Ecoinvent database
CO_2 [kg]	Determined by the electricity consumption of the compression stage	CO_2 capture using MEA as solvent. The impact embodied in the electricity consumed by the compressors is already accounted for in the value reported in the database.
Hydrogen [kg]	3.09	Market for hydrogen. Impacts embodied correspond to the mix of current technologies.
Steam [kg × 1000]	14.3	Steam production in the chemical industry
Electricity [MW]	94.5	High voltage electricity mix
Cooling water [m^3]	0.03	Tap water production, conventional treatment
Catalyst [kg]	95.24	Not considered
Steel [kg]	Capital costs	Steel production chromium steel 18/8
Heat recovery [kg × 1000]	7.7	Steam production in chemical industry
Wastewater treatment [m^3]	1.5	Treatment of wastewater

gate are fixed and its results are compared against the data of the original model. After building and testing the surrogate, we evaluated the relative error for the entire set of feasible solutions used in building the model, which in this case was below the minimum allowable tolerance of 10%. Hence, the surrogate was next used in the objective reduction stage. We note that the evaluation of the surrogate is significantly faster than running the Aspen-HYSYS model: the lowest time per evaluation in Aspen-HYSYS was 4 s, which went up to 198 s for non-converged designs; meanwhile, the average time per evaluation of the surrogate was below 0.005 s.

As shown in Fig. 2, the building of the surrogate involves an iterative procedure that ends when the desired error tolerance is achieved. In our case, despite attaining the required accuracy in one step, the surrogate was re-calibrated twice to improve the quality of the predictions made near the optimal solution of the model. To do so, we generated a second set of samples (Z_2) optimizing the surrogate separately for each objective using a single-objective genetic algorithm. The optimization of each objective was performed 10 times to generate a total of 110 samples. The results of the optimization were tested in the original model in Aspen-HYSYS and resulted in 91 converged simulations out of which 85 were feasible. These 85 samples were added to the original 209 feasible samples obtained from Z_1 and the surrogate was then re-calibrated. As in the first iteration, 70% of the samples were used to train the model, 15% to validate it and 15% to test it. The relative error for the entire set of feasible solutions (209 + 85) was then calculated.

The final calibration of the surrogate was made using a third set of samples (Z_3) obtained by executing the MOGA five times. After this procedure, we obtained a total of 91 solutions, out of which 83 converged and 79 were feasible after being evaluated in Aspen-HYSYS. This set of feasible solutions was added to the previous data and used to re-calibrate the surrogate in a similar way as was done in the previous iterations. The relative error for the entire set of feasible solutions (209 + 85 + 79) was finally calculated. In the final results retrieved from the MOGA, a total of 137 optimal points were generated. Among them, 126 converged and all of them satisfied the productivity constraint. The simulation in Aspen-HYSYS was evaluated a total of 1338 times until we obtained the final Pareto frontier. To generate the surrogate, a total of 373 feasible samples were used (209 from Z_1, 85 from Z_2 and 79 from Z_3).The relative error of the surrogate for the final evaluation was below 5%.

Step 2.1 Objective reduction. The objective reduction step requires an initial approximation of the Pareto frontier. To build this approximation, we generated an initial set of points using a single-objective genetic algorithm coupled with the surrogate model and optimizing the 11 objectives separately. In the genetic algorithm, the initial population "evolves" according to the ranking of individuals at each generation and following mutation and crossover procedures, which leads to different solutions in different runs (Coello Coello et al., 2007). To produce more consistent results, we ran the single-objective genetic algorithm 10 times for each objective. The set of decision variables obtained in the single-objective optimizations ($Z_2 = 110$) was tested in the original model and the best solutions for each objective were then used to build the initial Pareto frontier S_0 required for the objective reduction algorithm. As previously described, the solutions of the simulation in Aspen-HYSYS were used to re-calibrate the surrogate model (Fig. 7). After normalizing the Pareto frontier S_0 using Eq. (A1), we carried out the objective reduction by performing an exhaustive exploration of model A-P1 for an approximation error $\bar{\delta} = 0$. The results of the MILP indicated that five objectives were required to ensure an approximation error of zero: TAC, GWP, EP, HT, and PO.

Step 2.2 Multi-objective optimization and comparison between the full-space and reduced-space models. The MOO of the surrogate model was performed using the MOGA algorithm already implemented in the MATLAB optimization toolbox ("Optimization Toolbox ™ User's Guide R2017b," 2017). The methanol production rate, which was the only additional constraint omitted in the simulation model, was handled by defining a slack variable and a penalty term in the objective function. During the optimization, we first ran the MOO algorithm in the reduced space to re-calibrate the surrogate and then repeated the procedure to generate the final Pareto frontier. The MOGA was set with an initial population of 100 individuals and 1000 generations as stopping criterion. We included as initial population the 85 feasible points obtained in the single-objective optimizations. The MOGA was executed five times and a total of 91 non-repeated solutions were obtained (Z_3). This set of solutions was evaluated in Aspen-HYSYS and resulted in 79 feasible samples, which were used to re-calibrate the surrogate. After the fitting of the surrogate, we

Table 4 – Lower and upper bound for the solutions contained in the final Pareto frontier. [Units per kg of methanol produced. LB: Lower bound; UB: Upper bound].

Reduced space

	TAC (€)	GWP (kg CO_2-eq)	EP (kg PO_4-eq)	HT(kg 1,4-DCB-eq)	PO (kg C_2H_4-eq × 10^{-3})
LB	0.767	−0.029	0.020	2.013	1.09
UP	0.847	0.142	0.132	2.198	8.83

Omitted objectives

	AP (kg SO_2-eq) × 10^{-3}	DAR (kg Sb-eq) × 10^{-2}	FAET (kg 1,4-DCB-eq)	MAET (kg 1,4-DCB-eq)	TE (kg 1,4-DCB-eq × 10^{-3})	OLD (kg CFC-11-eq × 10^{-7})
LB	4.42	1.18	0.42	1451	4.27	1.31
UB	5.23	1.33	0.49	1682	4.90	1.53

solved five more times the MOGA in the reduced space using the same initial population and stopping criterion, resulting in 137 non-repeated solutions. Among them, 126 points converged and all of them were feasible in the original model in Aspen-HYSYS. The summary of both evaluations is shown in Fig. 7 and the boundaries of the final Pareto frontier are presented in Table 4.

The sampling was the most time consuming part of the methodology, where a total of 15 h were required to evaluate the 1338 samples in Aspen-HYSYS (≈40 s on average per evaluation). The building and re-calibration of the surrogate required approximately 300 s in total (≈100 s per iteration). The single objective optimizations required a total of ≈330 s while the MOGA used a total of ≈185 s for the five iterations previously described. The OR using the exhaustive exploration of model A-P1 required 190 s. The total time to generate the final Pareto frontier required 15 h for the evaluation of the original model plus ≈1000 s in building the surrogate, reducing objectives and optimizing the model. For comparison purposes, let us consider the same population size using the Aspen-HYSYS model coupled with the MOGA. If convergence was achieved in the same number of generations as in the surrogate (≈300 generations), a total of 30,000 simulations would have been required, resulting in approximately 330 h to obtain the Pareto solutions.

To further check if the use of fewer objectives in the MOO problem provided a real advantage, we compared the frontiers generated when optimizing the surrogate model for five (S_r) and eleven (S_f) objectives, respectively. The comparison was made using the hypervolume indicator (Zitzler and Thiele, 1998), which measures the area dominated by the Pareto optimal solutions considering a reference point. The larger the value of the hypervolume, the better the quality of the Pareto frontier. Fig. 8 shows the graphical representation of the hypervolume for two objectives.

In both, full and reduced spaces, the Pareto frontiers were generated using a MOGA having an initial random population of 100 individuals and 1000 generations as stopping criteria. To calculate the hypervolume, we used the approximation developed by Everson et al. (2002), which is based on Monte Carlo sampling. The MOGA was run five times for each case, while the hypervolume was calculated after the five iterations. This approach was repeated ten times to ensure the consistency of the results. The results are shown in Table 5, where we present the hypervolume indicator for both frontiers and the average time spent by the MOGA to provide the Pareto frontier. The advantage of reducing objectives when using MOGA is twofold: the quality of the Pareto frontier improves while the time spent in the optimization drops (Deb and Saxena, 2006). This is shown in Table 5, where the average computational time

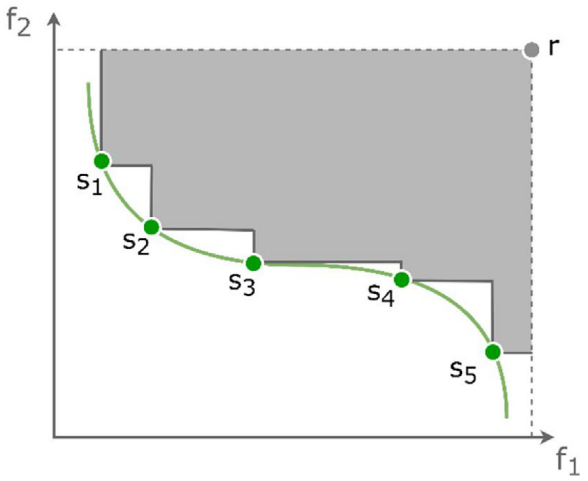

Fig. 8 – Graphical representation of the hypervolume indicator for two dimensions. The hypervolume corresponds to the area enclosed by the frontier considering the reference point r.

to generate the approximation of the Pareto frontier considering a given stopping criterion is slightly lower in the reduced space. In terms of the quality of the Pareto frontier measured by the hypervolume, it is clear that the reduced space S_r yields always a better non-dominated front compared to the original space S_f model. This results clearly justify the additional effort spent during the objective-reduction stage.

Step 3: Post-analysis of the Pareto frontier using DEA. The solutions obtained from the MOGA were ranked using the super-efficiency concept. To this end, we first normalized the 126 points that converged in Aspen-HYSYS including the base case design (BC) taken from Pérez-Fortes et al. (2016) The normalization was performed using Eq. (A2) and the DEA analysis was carried out in the reduced space modeling the five objectives as inputs, as we aim to minimize them all. As output, we considered the production of 1 kg of methanol.

After solving model P4, only ten out of the 126 optimal points were found to be efficient, including the base case (s_{A1} to s_{A9} and BC). As we can see from the results, a significant number of solutions were ruled out by applying the concept of efficiency in DEA, as they did not belong to the convex envelop of the efficient frontier. The values for the efficient solutions obtained using model P4 are shown in Fig. 9. As we can see, design BC was also identified as efficient because it showed the lowest impact value among the 127 designs in the category of photochemical oxidation (PO).

To further rank the efficient solutions, we calculated the super-efficiency score by solving model P4 including Eqs. (3) and (4). The ranking of the efficient solutions is shown in

Table 5 – Hypervolume indicator evaluated for the Pareto frontiers of the original and reduced space.

MOGA	Time[a] (s)	HVI avg.	1	2	3	4	5	6	7	8	9	10
Full domain S_f (11 objectives)	37.9	4.4	1.99	5.72	2.82	3.27	6.48	5.8	10.1	2.5	1.36	4.41
Reduced space S_r (5 objectives)	37.0	10.2	6.58	7.36	7.03	6.97	16.4	19.3	13.6	2.6	5.11	17.3

[a] Time to run the MOGA having a population of 100 individuals and 1000 generations as stopping criterion. Solution was reached before the stopping criterion of maximum number of generations in all the cases.

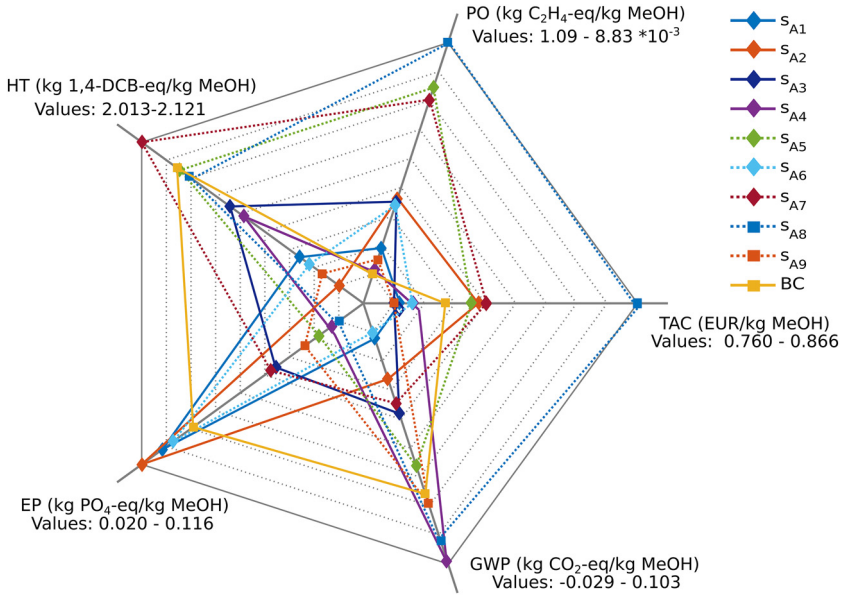

Fig. 9 – Values for the efficient units and case BC in the reduced space without constraints on the weights.

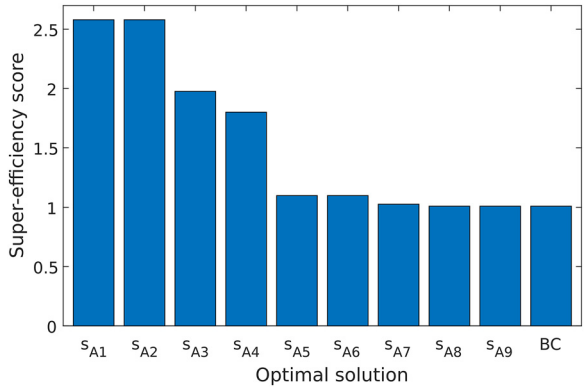

Fig. 10 – Super-efficiency score for the efficient designs S_A.

Fig. 10. In this case, the super-efficiency provided the same score for designs s_{A1} and s_{A2}, while the rest showed significantly lower super-efficiency values. From Fig. 9, we can see that these two designs had a similar performance in the TAC, HT and PO categories, while their impact in the EP and GWP categories significantly differed from each other. From Fig. 10, we can also see how the base case showed the lowest super-efficiency score, indicating that better designs were possible.

The super-efficiency concept allows ranking alternatives based on the shape of the Pareto front. This ranking, however, does not reflect any order of preferences. An alternative approach to narrow down further the set of Pareto points (see Section 2.3) is to include additional constraints on P3 reflecting priorities in the indicators. To exemplify this capability, we included the following constraint on the input multipliers v_l, which reflects a ranking of objectives from more to less important:

$$v_{GWP} \geq v_{TAC} \geq v_{HT} \geq v_{EP} \geq v_{PO} \quad (5)$$

That is, we sorted the objectives from the most important (GWP) to the least one (PO). From the total of 127 designs used in the analysis, the solution of the primal model P3 including Eq. (5) indicated that only four designs were efficient in the reduced space. Fig. 11 shows the values of the five objectives kept in the reduced space for the new efficient designs (i.e. those emerging as efficient when the constraints on weights are applied), and for the BC alternative. In this new analysis that imposed bounds on the weights, the base case became inefficient, displaying an efficiency score $\theta_{BC} = 0.53$. Reductions in the number of efficient solutions typically occurr when constraints of this type are introduced in the model, as they restrict the efficient frontier (Cook and Seiford, 2009).

From the results of model P3, we can also see that design BC is now identified as inefficient. This is explained by the fact that in Eq. (5) the category PO, where BC performed extremely well, is given the lowest priority. As a result, the high impact value for the remaining categories prevented this design from becoming efficient when the new constraints on weights were added.

To calculate the improvement targets for the BC design, we solved model P4. To include constraint Eq. (5) in the dual model P4, it is necessary to determine an Assurance Region (AR) (Cook and Seiford, 2009), defined as the feasible region in which the multipliers u_r and v_l will satisfy the equation. In our case, we applied the cone-ratio method (Thompson et al., 1995), where a polyhedral convex cone is defined to restrict the efficient frontier. The concept of cone-ratio method is shown in Fig. 12. This cone is expressed as a matrix D, which contains

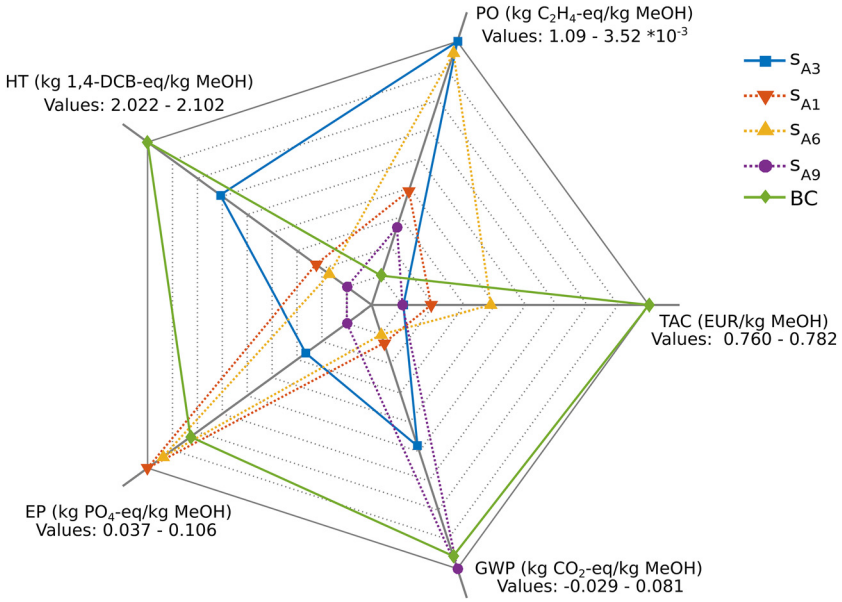

Fig. 11 – Values for the efficient units and BC in the reduced space using constraints on weights.

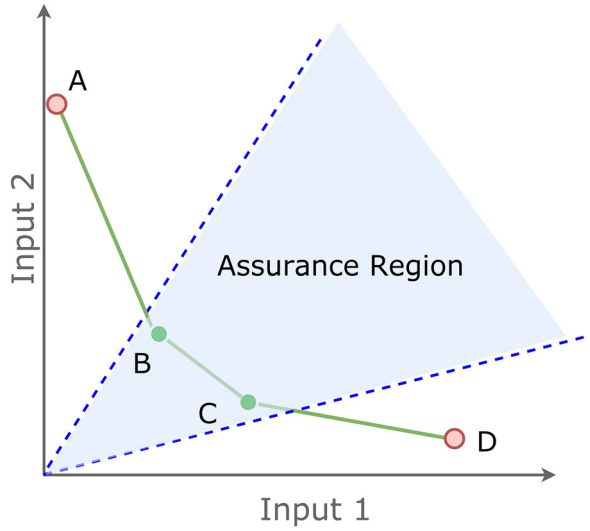

Fig. 12 – Graphical representation of the assurance region. The assurance region is determined by the blue region and reflects the preferences on the multipliers. Units falling out of the efficient frontier contained in the assurance region are inefficient. This also applies to units identified as efficient by model P3 without considering the assurance region, such as units A and D.

the preferences on the multipliers and modifies the original inputs and outputs:

$$D = \begin{pmatrix} A & 0 \\ 0 & B \end{pmatrix} \tag{6}$$

Where A defines the constraints imposed on the multipliers of inputs x_{io}, while B defines constraints imposed on the multipliers of outputs y_{ro}. The cone-ratio, expressed as matrix D, is further used to transform the original inputs and outputs of the model as follows:

$$D\begin{pmatrix} x_{io} \\ y_{ro} \end{pmatrix} = \begin{pmatrix} Ax_{io} \\ By_{ro} \end{pmatrix} = \begin{pmatrix} \bar{X} \\ \bar{Y} \end{pmatrix} \tag{7}$$

In our case, matrix D was built by using the optimal multipliers of the efficient units identified using model P3(Cooper et al., 2006):

$$D = \begin{pmatrix} 1 & 0 & 0 & 0 & 0 & 0 \\ 0 & 1.158 & 1.158 & 0.917 & 0.917 & 0.917 \\ 0 & 2.075 & 2.075 & 0.969 & 0.969 & 0.0 \\ 0 & 7.107 & 10.067 & 0.0 & 7.107 & 0.0 \\ 0 & 1.164 & 1.164 & 1.067 & 1.067 & 0.0 \end{pmatrix} \tag{8}$$

By substituting Eq. (8) in Eq. (7), the original inputs x_{io} and outputs y_{ro} were transformed into $\bar{X}$ and $\bar{Y}$, respectively. Model P4 was then solved by replacing x_{io} and y_{ro} by $\bar{X}$ and $\bar{Y}$. In the absence of Eq. (5), the improvement targets are calculated solving model P4 with the original inputs and outputs and the AR is not required. The solution of model P4 for $\bar{X}$ and $\bar{Y}$ indicated that the inputs of design BC should be reduced to the level of solution s_{A1} ($y_{BC} = 1 \times y_{SA1}$). The reason why only one efficient unit was used to improve BC is that its projection onto the efficient frontier of the AR falls in the weakly efficient frontier (Fig. 4). Therefore, the closest design in the efficient frontier was solution s_{A1}.

Typically, the improvement targets obtained from DEA in an input-oriented model will imply reductions in the value of all the inputs (Cook and Seiford, 2009). However, this is not always the case when constraints on multipliers are included, as the efficient frontier is modified in order to fulfill such constraints. Particularly, the targets for the BC design entail that the TAC needs to be reduced by 1.84% (from 0.782 to 0.768 €/kg_{MeOH}), GWP by 134% (from 0.07 to −0.03 kg CO_2 eq/kg_{MeOH}), and HT by 3.5% (from 2.10 to 2.03 kg 1,2-DCB eq/kg_{MeOH}). Conversely, the categories of EP and PO showed an increase by 10% (from 0.09 to 0.10 kg PO_4 eq/kg_{MeOH}) and 211% (from 0.001 to 0.003 kg C_2H_4 eq/kg_{MeOH}), respectively. Note that this does not imply that the BC design needs to worsen its performance in the latter categories (EP and PO), but rather that there is room for doing so while still being efficient when attempting to attain the targets on the TAC, GWP and HT. An analysis of the decision variables values in the peers and how they impact the sustainability indicators provides further insight on how to achieve these targets in practice. In this case, the decision variables values

in design BC would have to approach as much as possible those in design s_{A1}, as it was the unique peer identified.

Coming back to the best solutions calculated in the super-efficiency assessment, we found that hydrogen was the main contributor to the total value of the TAC (≈80%), while CO_2 was the main contributor in HT (≈90%). The reason for such a large contribution of CO_2 in the HT category is the use of solvents during the carbon capture process. In the case of GWP, hydrogen contributes with 0.42 kg CO_2-eq per kg of methanol, while in the case of CO_2 this value is −0.46 kg CO_2-eq per kg of methanol. The remaining impact is equally attributed to cooling water, heat recovery and emissions (≈0.40 kg CO_2-eq per kg of methanol in each case).

The impacts in the categories of EP and PO were mainly caused by the emissions generated in the process (>90% and >70%, respectively). Note that, to reduce the impact, part of the purge shall be emitted to the atmosphere without any combustion. The reason for this is that when the purge is burned, the methanol contained in the stream is transformed into CO_2, thereby increasing the GWP indicator. On the other hand, if methanol is released in the purge stream, the PO indicator increases while the GWP decreases. This also explains why design BC had the lowest value in the PO category, as it was the only option where the purge was fully combusted. We also identified the recycling ratio as one of the main decision variables of the process, with strong links to the flow rates of CO_2 and H_2 and the size of the equipment units. That is, when the recycling ratio was below 99.5%, the flow rate of raw materials increased while the size of the reactor and distillation column decreased. This was the case for designs s_{A1}, s_{A2}, s_{A3}, s_{A5}, s_{A6}, s_{A7}, and BC. For values above 99.5%, a lower flow rate of raw materials was required, yet the reactor and distillation column should be increased in size to reach the production rate sought. Finally, the full methodology of SUSCAPE pointed design s_{A1} and s_{A2} as the most sustainable options when no constraints were included on the indicators. The main difference between both designs was the higher consumption of H_2 in design s_{A2} (5661 kg/h in s_{A2}versus 5460 kh/h in s_{A1}). An additional difference between these designs was the inlet temperature of the distillation column, raising from 75 °C in s_{A1} to 86 °C in s_{A2}. Finally, the higher consumption of hydrogen in s_{A2} caused the TAC indicator to increase, making this design inefficient when constraints in the multipliers were included.

4. Conclusions

We introduced a framework for the optimal design of sustainable chemical processes that combines life cycle assessment principles, surrogate modeling, objective reduction techniques, multi-objective optimization and DEA. What really makes our framework unique, besides the integration of the aforementioned tools within a single unified approach, is the application of DEA to facilitate the post-optimal analysis of the Pareto points. The framework presented was applied to the production of methanol from CO_2 and hydrogen. The use of a surrogate model allowed to reduce the time spent in evaluating and optimizing the model. Furthermore, eliminating objectives reduced the time spent in obtaining the Pareto front while increasing its quality during the execution of the MOO algorithm. Finally, the application of DEA allowed us to narrow down the number of Pareto points and to establish improvement targets for a base case design showing worst performance.

Future work should focus on incorporating the social dimension of sustainability together with the main uncertainties affecting the calculations. Similarly, the use and optimization of more rigorous models should be incorporated in macro-scale analyses of the chemical industry. In these terms, our framework can also benefit from further developments in each of the areas and tools that it incorporates, including surrogate modeling, objective reduction and core methodologies for process design. Finally, contributions such as the one presented in this work will facilitate the development of a sustainable chemical industry by assessing new processes and technologies and also by identifying improvement targets for current suboptimal technologies.

Acknowledgments

Gonzalo Guillén-Gosálbez would like to acknowledge the financial support received from the Spanish “Ministerio de Ciencia y Competitividad” through the project CTQ2016-77968-C3-1-P.

Andres Gonzalez-Garay acknowledge the financial support granted by the Mexican “Consejo Nacional de Ciencia y Tecnologia (CONACyT)”.

Appendix A. : Objective reduction (OR)

In OR approaches, redundant objectives are identified by quantifying a minimum approximation error using an initial approximation of the whole Pareto frontier. This initial frontier can be typically constructed in several ways. One possible manner to generate this approximation to the frontier is to run single-objective optimizations for each metric separately and then use the extreme points obtained. Another possible way is to generate points in the space of every combination of two objectives. After the approximation of the Pareto frontier is obtained and prior to the application of the OR model, a normalization step is carried out to improve the numerical performance of the OR algorithm according to the following expressions:

$$f_{ni} = (f_i - f_{imin}) / (f_{imax} - f_{imin}) \quad \text{(A1)}$$

$$f_{ni} = (f_{imax} - f_i) / (f_{imax} - f_{imin}) \quad \text{(A2)}$$

Where f_{ni} represents a normalized value in objective i, and f_{imax} and f_{imin} represent the maximum and minimum values of objective i, respectively. Eq. (A1) is used for those objectives to be minimized, while Eq. (A2) is employed for objectives to be maximized.

The OR method seeks to identify a subset of objectives k from the full space K ($k \subseteq K$) such that the dominance structure of the Pareto front is preserved within a minimum allowable error. We next provide an overview of the MILP, while further details can be found in Guillén-Gosálbez (2011).

The MILP carries out a dimensionality reduction analysis for an initial set of Pareto points p belonging to the set P and considering $|K|$ objectives, some of which will be omitted based on an error metric. To evaluate the approximation error incurred when removing objectives, that is, when producing the Pareto front of dimension k instead of the original one containing $|K|$ criteria ($k < K$), we define the binary parameter $YP_{p,p',i}$ and the binary variables ZO_i and $ZD_{p,p'}$. $YP_{p,p',i}$ models the dominance relationship between solutions p and p′ in

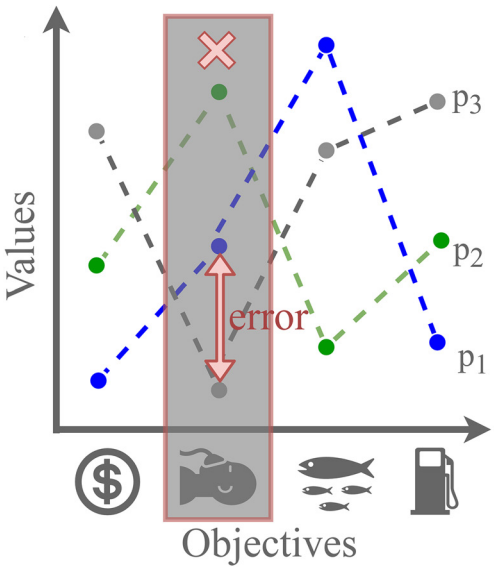

$Y_{p,p',i}$					
i / p,p	1	2	3	4	$ZD_{p,p'}$
1,2	1	1	0	1	0
1,3	1	0	0	1	0
2,1	0	0	1	0	0
2,3	1	0	1	1	0
3,1	0	1	1	0	0
3,2	0	1	0	0	1
ZO_i	0	1	0	0	

Fig. A1 – Notation used in objective reduction model.

objective i, and takes the value of one if solution p is better than solution p' in objective i and zero otherwise. ZO_i models the decision of eliminating objectives from the original space, and is one if objective i is removed and zero if it remains in the set. $ZD_{p,p'}$ models the dominance relationship between solutions p and p' in the reduced space, and is one if solution p' dominates p in the reduced Pareto space (after removing objectives) and zero otherwise.

This notation is clarified in Fig. A1, where three optimal solutions are considered for a problem with four objectives. In this example, objective two is removed from the original space, resulting in $ZO_2 = 1$. Fig. A1 also shows how solution p_2 dominates solution p_3 in the reduced space, which results in $ZD_{3,2} = 1$. This does not happen in the original space, where p_3 is Pareto optimal due to its good performance in objective 2. Furthermore, the values of the binary parameter $YP_{p,p',i}$ are presented in the table attached to the figure.

In essence, the MILP seeks to minimize the approximation error of removing objectives from the original space. This error is quantified by the variable $\delta_{p,p',i}$, which quantifies the maximum difference in the removed objective i between solutions p' (e.g., p_2) and p (e.g., p_3), where the former dominates the latter in the reduced domain, such that p' would also dominate p in the original space. To clarify this, let us consider the example in Fig. A1. As previously described, solution p_2 dominates solution p_3 in the reduced space; however, this is not true when objective 2 is removed. For solution p_2 to dominate solution p_3 in the full space, the value of solution p_2 in objective 2 should be at least equal to the one in solution p_3. This difference between solutions p_2 and p_3 in objective 2 is employed to quantify the approximation error $\delta_{3,2,2}$. This error is calculated as follows:

$$\delta_{p,p,i} = \left(f_{p',i} - f_{p,i}\right) ZOD_{p,p',i} \forall p \neq p' \quad \text{(A3)}$$

Where $ZOD_{p,p',i}$ is defined by the following constraints:

$$ZOD_{p,p',i} \leq ZO_i \quad \forall p \neq p' \quad \text{(A4)}$$

$$ZOD_{p,p,i'} \leq ZD_{p,p'} \quad \forall p \neq p' \quad \text{(A5)}$$

$$ZOD_{p,p',i} \geq ZO_i + ZD_{p,p'} - 1 \forall p \neq p' \quad \text{(A6)}$$

Using Eq. (A3), the value of $\delta_{p,p',i}$ is determined only for those solutions p dominated by at least another solution p' in the reduced space ($ZD_{p,p'} = 1$) and only when objective i is omitted ($ZO_i = 1$). In contrast, if solution s is not dominated in the reduced space ($ZD_{p,p'} = 0$) or objective i is not omitted ($ZO_i = 0$), then $\delta_{p,p',i}$ will take a zero value.

The definition of $ZD_{p,p'}$ is enforced by the following constraints:

$$(K - \sum ZO_i) - K(1 - ZD_{p,p'}) \leq \sum_i YP_{p',p,i}(1 - ZO_i) \leq (K - \sum ZO_i) + K(1 - ZD_{p,p'}) \forall p \neq p' \quad \text{(A7)}$$

$$\sum_i YP_{p',p,i}(1 - ZO_i) \leq (K - \sum_i ZO_i) - 1 + KZD_{p,p'} \quad \forall p \neq p' \quad \text{(A8)}$$

From Eq. (A7), if solution p is dominated by solution p' in the reduced space, the variable $YP_{p',p,i}$ will be equal to one for all the objectives kept in the reduced space ($ZO_i = 0$). In that case, the sum of $YP_{p',p,i}$ will be equal to the reduced number of objectives for which $ZD_{p,p'}$ equals one. If solution p is not dominated by solution p', the sum of $YP_{p',p,i}(1 - ZO_i)$ will be lower than the number of objectives kept and Eq. (A8) will force $ZD_{p,p'}$ to be equal to zero.

Considering that our goal is to identify the minimum number of objectives for a given error $\bar{\delta}$, we can impose an upper bound on $\delta_{p,p',i}$ as follows:

$$\delta_{p,p',i} \leq \bar{\delta} \quad \text{(A9)}$$

Finally, the MILP formulation can be expressed in compact form as follows:

$$\max \sum_i ZO_i \quad \text{(A-P1)}$$

s.t. constraints A3-A9.

The solution of this MILP provides the minimum combination of objectives for which $\delta_{p,p',i} \leq \bar{\delta}$. Note that additional constraints can be added to avoid calculating errors between

two solutions that are not Pareto optimal in the reduced space (see the original paper for details (Guillén-Gosálbez, 2011)).

Note that it may happen that the exhaustive exploration of all combinations of objectives may be faster than solving the MILP, particularly in cases where many objectives can be eliminated without increasing the approximation error.

References

Andersen, P., Petersen, N.C., 1993. A procedure for ranking efficient units in data envelopment analysis. Manage. Sci. 39, 1261–1264, http://dx.doi.org/10.1287/mnsc.39.10.1261.

Azapagic, A., Clift, R., 1999. Life cycle assessment and multiobjective optimisation. J. Clean Prod. 7, 135–143, http://dx.doi.org/10.1016/S0959-6526(98)00051-1.

Azapagic, A., 1999. Life cycle assessment and its application to process selection, design and optimisation. Chem. Eng. J. 73, 1–21, http://dx.doi.org/10.1016/S1385-8947(99)00042-X.

Azapagic, A., Stamford, L., Youds, L., Barteczko-Hibbert, C., 2016. Towards sustainable production and consumption: a novel decision-support framework integrating economic environmental and social sustainability (DESIRES). Comput. Chem. Eng. 91, 93–103, http://dx.doi.org/10.1016/j.compchemeng.2016.03.017.

Babi, D.K., Holtbruegge, J., Lutze, P., Gorak, A., Woodley, J.M., Gani, R., 2015. Sustainable process synthesis–intensification. Comput. Chem. Eng. 81, 218–244, http://dx.doi.org/10.1016/j.compchemeng.2015.04.030.

Banker, R.D., 1984. Estimating most productive scale size using data envelopment analysis. Eur. J. Oper. Res. 17, 35–44, http://dx.doi.org/10.1016/0377-2217(84)90006-7.

Bertran, M.-O., Frauzem, R., Sanchez-Arcilla, A.-S., Zhang, L., Woodley, J.M., Gani, R., 2017. A generic methodology for processing route synthesis and design based on superstructure optimization. Comput. Chem. Eng. 106, 892–910, http://dx.doi.org/10.1016/j.compchemeng.2017.01.030.

Biegler, L.T., Lang, Y.-D., Lin, W., 2014. Multi-scale optimization for process systems engineering. Comput. Chem. Eng. 60, 17–30, http://dx.doi.org/10.1016/j.compchemeng.2013.07.009.

Bortz, M., Burger, J., Asprion, N., Blagov, S., Bottcher, R., Nowak, U., Scheithauer, A., Welke, R., Kofer, K.-H., Hasse, H., 2014. Multi-criteria optimization in chemical process design and decision support by navigation on Pareto sets. Comput. Chem. Eng. 60, 354–363, http://dx.doi.org/10.1016/j.compchemeng.2013.09.015.

Boukouvala, F., Floudas, C.A., 2016. ARGONAUT: AlgoRithms for Global Optimization of coNstrAined grey-box compUTational problems. Optim. Lett. 11 (5), 895–913, http://dx.doi.org/10.1007/s11590-016-1028-2.

Boukouvala, F., Hasan, M.M.F., Floudas, C.A., 2015. Global optimization of general constrained grey-box models: new method and its application to constrained PDEs for pressure swing adsorption. J. Glob. Optim. 67, 3–42, http://dx.doi.org/10.1007/s10898-015-0376-2.

Boukouvala, F., Ierapetritou, M.G., 2013. Surrogate-based optimization of expensive flowsheet modeling for continuous pharmaceutical manufacturing. J. Pharm. Innov. 8, 131–145, http://dx.doi.org/10.1007/s12247-013-9154-1.

Brockhoff, D., Zitzler, E., 2006. Are all objectives necessary? On dimensionality reduction in evolutionary multiobjective optimization. Parallel Problem Solving from Nature — PPSN IX, 533–542, http://dx.doi.org/10.1007/11844297_54.

Brunet, R., Guillén-Gosálbez, G., Jiménez, L., 2012. Cleaner design of single-product biotechnological facilities through the integration of process simulation, multiobjective optimization, life cycle assessment, and principal component analysis. Ind. Eng. Chem. Res. 51, 410–424, http://dx.doi.org/10.1021/ie2011577.

Burger, J., Asprion, N., Blagov, S., Böttcher, R., Nowak, U., Bortz, M., Welke, R., Küfer, K.-H., Hasse, H., 2014. Multi-objective optimization and decision support in process engineering — implementation and application. Chem. Ing. Tech. 86, 1065–1072, http://dx.doi.org/10.1002/cite.201400008.

Caballero, J.A., Grossmann, I.E., 2008. An algorithm for the use of surrogate models in modular flowsheet optimization. AIChE J. 54, 2633–2650, http://dx.doi.org/10.1002/aic.

Caballero, J.A.J.A., Milán-Yañez, D., Grossmann, I.E., 2005. Rigorous design of distillation columns: integration of disjunctive programming and process simulators. Ind. Eng. Chem. Res. 44, 6760–6775, http://dx.doi.org/10.1021/ie050080l.

Calvo-Serrano, R., Guillen-Gosalbez, G., 2018. Streamlined life cycle assessment under uncertainty integrating a network of the petrochemical industry and optimization techniques: ecoinvent vs mathematical modeling. ACS Sustain. Chem. Eng. 6, 7109–7118, http://dx.doi.org/10.1021/acssuschemeng.8b01050.

Carvalho, A., Mimoso, A.F., Mendes, A.N., Matos, H.A., 2014. From a literature review to a framework for environmental process impact assessment index. J. Clean. Prod. 64, 36–62, http://dx.doi.org/10.1016/j.jclepro.2013.08.010.

Charnes, A., Cooper, W.W., Rhodes, E., 1978. Measuring the efficiency of decision making units. Eur. J. Oper. Res. 2, 429–444, http://dx.doi.org/10.1016/0377-2217(78)90138-8.

Coello Coello, C.A., Lamont, G.B., Van Veldhuizen, D.A., 2007. Evolutionary Algorithms for Solving Multi-Objective Problems, 2nd ed. Springer, http://dx.doi.org/10.1007/978-0-387-36797-2.

Cook, W.D., Seiford, L.M., 2009. Data envelopment analysis (DEA) — thirty years on. Eur. J. Oper. Res. 192, 1–17, http://dx.doi.org/10.1016/j.ejor.2008.01.032.

Cooper, W.W., Seiford, L.M., Tone, K., 2006. Introduction to Data Envelopment Analysis and Its Uses: With DEA-Solver Software and References. Springer Science+Business Media Inc.

Cozad, A., Sahinidis, N.V., Miller, D.C., 2014. Learning surrogate models for simulation-based optimization. AIChE J. 60, 2211–2227, http://dx.doi.org/10.1002/aic.

Deb, K., Saxena, D.K., 2006. Searching for pareto-optimal solutions through dimensionality reduction for certain large-dimensional multi-objective optimization problems. IEEE Congress on Evolutionary Computation, 3353–3360, IEEE Computer Society Press.

Dreyer, L.C., Niemann, A.L., Hauschild, M.Z., 2003. Comparison of three different LCIA methods: EDIP97, CML2001 and Eco-indicator 99. Int. J. Life Cycle Assess. 8, 191–200, http://dx.doi.org/10.1007/BF02978471.

Everson, R.M., Fieldsend, J.E., Singh, S., 2002. Full elite sets for multi-objective optimisation. In: Adaptive Computing in Design and Manufacture V. Springer London, London, pp. 343–354, http://dx.doi.org/10.1007/978-0-85729-345-9_29.

Galán-Martín, Á., Guillén-Gosálbez, G., Stamford, L., Azapagic, A., 2016. Enhanced data envelopment analysis for sustainability assessment: a novel methodology and application to electricity technologies. Comput. Chem. Eng. 90, 188–200, http://dx.doi.org/10.1016/j.compchemeng.2016.04.022.

Gong, J., You, F., 2017. Consequential life cycle optimization: general conceptual framework and application to algal renewable diesel production. ACS Sustain. Chem. Eng. 5, 5887–5911, http://dx.doi.org/10.1021/acssuschemeng.7b00631.

Grossmann, I.E., Guillen-Gosalbez, G., 2010. Scope for the application of mathematical programming techniques in the synthesis and planning of sustainable processes. Comput. Chem. Eng. 34, 1365–1376, http://dx.doi.org/10.1016/j.compchemeng.2009.11.012.

Guillén-Gosálbez, G., 2011. A novel MILP-based objective reduction method for multi-objective optimization: application to environmental problems. Comput. Chem. Eng. 35, 1469–1477, http://dx.doi.org/10.1016/j.compchemeng.2011.02.001.

Guillén-Gosálbez, G., Caballero, J.A., Jiménez, L., 2008. Application of life cycle assessment to the structural optimization of process flowsheets. Ind. Eng. Chem. Res. 47, 777–789, http://dx.doi.org/10.1021/ie070448+.

Helmdach, D., Yaseneva, P., Heer, P.K., Schweidtmann, A.M., Lapkin, A.A., 2017. a multiobjective optimization including results of life cycle assessment in developing

biorenewables-based processes. ChemSusChem 10, 3632–3643, http://dx.doi.org/10.1002/cssc.201700927.
Himmelblau, D.M., 2008. Accounts of experiences in the application of artificial neural networks in chemical engineering. Ind. Eng. Chem. Res., http://dx.doi.org/10.1021/ie800076s.
Huang, I.B., Keisler, J., Linkov, I., 2011. Multi-criteria decision analysis in environmental sciences: ten years of applications and trends. Sci. Total Environ. 409, 3578–3594, http://dx.doi.org/10.1016/j.scitotenv.2011.06.022.
Hui Liew, W., Hassim, M.H., Ng, D.K., 2016. Systematic framework for sustainability assessment on chemical production pathway: basic engineering stage. Process Saf. Environ. Prot. 1, 161–177, http://dx.doi.org/10.1016/j.psep.2016.08.009.
Hui Liew, W., Hassim, M.H., Ng, D.K.S., Chemmangattuvalappil, N., 2015. Systematic framework for sustainability assessment of biodiesel production: preliminary engineering stage. Ind. Eng. Chem. Res. 54, 12615–12629, http://dx.doi.org/10.1021/acs.iecr.5b02894.
Ibrahim, D., Jobson, M., Guillén-Gosálbez, G., 2017. Optimization-based design of crude oil distillation units using rigorous simulation models. Ind. Eng. Chem. Res. 56, 6728–6740, http://dx.doi.org/10.1021/acs.iecr.7b01014.
ISO, 2006. ISO 14040. Euro code SS-EN-1191-2.
Jacquemin, L., Pontalier, P.-Y., Sablayrolles, C., 2012. Life cycle assessment (LCA) applied to the process industry: a review. Int. J. Life Cycle Assess. 17, 1028–1041, http://dx.doi.org/10.1007/s11367-012-0432-9.
Khila, Z., Baccar, I., Jemel, I., Houas, A., Hajjaji, N., 2016. Energetic, exergetic and environmental life cycle assessment analyses as tools for optimization of hydrogen production by autothermal reforming of bioethanol. Int. J. Hydrogen Eergy 41, 17723–17739, http://dx.doi.org/10.1016/j.ijhydene.2016.07.225.
Konak, A., Coit, D.W., Smith, A.E., 2006. Multi-objective optimization using genetic algorithms: a tutorial. Reliab. Eng. Syst. Saf. 91, 992–1007, http://dx.doi.org/10.1016/j.ress.2005.11.018.
Korhonen, P.J., Luptacik, M., 2004. Eco-efficiency analysis of power plants: an extension of data envelopment analysis. Eur. J. Oper. Res. 154, 437–446, http://dx.doi.org/10.1016/S0377-2217(03)00180-2.
Li, M.-J., Tao, W.-Q., 2017. Review of methodologies and polices for evaluation of energy efficiency in high energy-consuming industry. Appl. Energy 187, 203–215, http://dx.doi.org/10.1016/j.apenergy.2016.11.039.
Lin, Z., Wang, J., Nikolakis, V., Ierapetritou, M., 2017. Process flowsheet optimization of chemicals production from biomass derived glucose solutions. Comput. Chem. Eng. 102, 258–267, http://dx.doi.org/10.1016/J.COMPCHEMENG.2016.09.012.
Lozano, S., Iribarren, D., Moreira, T., Feijoo, G., 2008. A joint application of life cycle assessment and data envelopment analysis. Sci. Total Environ. 407, 1744–1754, http://dx.doi.org/10.1016/j.scitotenv.2008.10.062.
Mckay, A.M.D., Beckman, R.J., Conover, W.J., 1979. A comparison of three methods for selecting values of input variables in the analysis of output from a computer code. Technometrics 21, 239–245.
Miettinen, P., Hämäläinen, R.P., 1997. How to benefit from decision analysis in environmental life cycle assessment (LCA). Eur. J. Oper. Res. 102, 279–294, http://dx.doi.org/10.1016/S0377-2217(97)00109-4.
Mio, A., Limleamthong, P., Guillen Gosalbez, G., Fermeglia, M., 2018. Sustainability evaluation of alternative routes for fine chemicals production in an early stage of process design adopting process simulation along with data envelopment analysis. Ind. Eng. Chem. Res., http://dx.doi.org/10.1021/acs.iecr.7b05126.
Narodoslawsky, M., 2013. Chemical engineering in a sustainable economy. Chem. Eng. Res. Des. 91, 2021–2028, http://dx.doi.org/10.1016/j.cherd.2013.06.022.
Nascimento, C.A.O., Giudici, R., Guardani, R., 2000. Neural network based approach for optimization of industrial chemical processes. Comput. Chem. Eng. 24, 2303–2314, http://dx.doi.org/10.1016/S0098-1354(00)00587-1.
Nikolopoulou, A., Ierapetritou, M.G., 2012. Optimal design of sustainable chemical processes and supply chains: a review. Comput. Chem. Eng. 44, 94–103, http://dx.doi.org/10.1016/j.compchemeng.2012.05.006.
Optimization Toolbox ™ User's Guide R2017b, 2017.
Otte, D., Lorenz, H.-M., Repke, J.-U., 2016. A toolbox using the stochastic optimization algorithm MIPT and ChemCAD for the systematic process retrofit of complex chemical processes. Comput. Chem. Eng. 84, 371–381, http://dx.doi.org/10.1016/J.COMPCHEMENG.2015.08.023.
Pattison, R.C., Tsay, C., Baldea, M., 2017. Pseudo-transient models for multiscale, multiresolution simulation and optimization of intensified reaction/separation/recycle processes: Framework and a dimethyl ether production case study. Comput. Chem. Eng. 105, 161–172, http://dx.doi.org/10.1016/j.compchemeng.2016.12.019.
Pérez-Fortes, M., Schöneberger, J.C., Boulamanti, A., Tzimas, E., 2016. Methanol synthesis using captured CO_2 as raw material: techno-economic and environmental assessment. Appl. Energy 161, 718–732, http://dx.doi.org/10.1016/j.apenergy.2015.07.067.
Quirante, N., Caballero, J.A., Grossmann, I.E., 2017. A novel disjunctive model for the simultaneous optimization and heat integration. Comput. Chem. Eng. 96, 149–168, http://dx.doi.org/10.1016/j.compchemeng.2016.10.002.
Quirante, N., Javaloyes, J., Caballero, J.A., 2015a. Rigorous design of distillation columns using surrogate models based on kriging interpolation. AIChE J. 61, 2169–2187, http://dx.doi.org/10.1002/aic.14798.
Quirante, N., Javaloyes, J., Ruiz-Femenia, R., Caballero, J.A., 2015b. Optimization of chemical processes using surrogate models based on a kriging interpolation. Comput. Aided Chem. Eng., http://dx.doi.org/10.1016/B978-0-444-63578-5.50025-6, Elsevier.
Ruiz-Mercado, G.J., Carvalho, A., Cabezas, H., 2016. Using green chemistry and engineering principles to design assess, and retrofit chemical processes for sustainability. ACS Sustain. Chem. Eng. 4, 6208–6221, http://dx.doi.org/10.1021/acssuschemeng.6b02200.
Seider, W.D., Seader, J.D., Lewin, D.R., Widagdo, S., 2009. Product and Process Design Principles: Synthesis, Analysis, and Evaluation, 3rd ed. John Wiley & Sons, US.
Serna, J., Díaz Martinez, E.N., Narváez Rincón, P.C., Camargo, M., Gálvez, D., Orjuela, Á., 2016. Multi-criteria decision analysis for the selection of sustainable chemical process routes during early design stages. Chem. Eng. Res. Des. 113, 28–49, http://dx.doi.org/10.1016/j.cherd.2016.07.001.
Sheldon, R.A., 2018. Metrics of green chemistry and sustainability: past present, and future. ACS Sustain. Chem. Eng. 6, 32–48, http://dx.doi.org/10.1021/acssuschemeng.7b03505.
Siew Ng, K., Martinez Hernandez, E., 2016. A systematic framework for energetic, environmental and economic (3E) assessment and design of polygeneration systems. Chem. Eng. Res. Des. 106, 1–25, http://dx.doi.org/10.1016/j.cherd.2015.11.017.
Skiborowski, M., Rautenberg, M., Marquardt, W., 2015. A hybrid evolutionary-deterministic optimization approach for conceptual design. Ind. Eng. Chem. Res. 54, 10054–10072, http://dx.doi.org/10.1021/acs.iecr.5b01995.
Smith, R., 2005. Chemical Process Design and Integration. John Wiley & Sons Ltd., http://dx.doi.org/10.1529/biophysj.107.124164.
Steimel, J., Engell, S., 2016. Optimization-based support for process design under uncertainty: a case study. AIChE J. 62, 3404–3419, http://dx.doi.org/10.1002/aic.
Steinmann, Z.J.N.N., Schipper, A.M., Hauck, M., Huijbregts, M.A.J.J., 2016. How many environmental impact indicators are needed in the evaluation of product life cycles? Environ. Sci. Technol. 50, 3913–3919, http://dx.doi.org/10.1021/acs.est.5b05179.

Sueyoshi, T., Yuan, Y., Goto, M., 2017. A literature study for DEA applied to energy and environment. Energy Econ. 62, 104–124, http://dx.doi.org/10.1016/j.eneco.2016.11.006.

Thompson, R.G., Dharmapala, P., Thrall, R.M., 1995. Linked-cone DEA profit ratios and technical efficiency with application to Illinois coal mines. Int. J. Prod. Econ. 39, 99–115, http://dx.doi.org/10.1016/0925-5273(94)00064-H.

Towler, G.P., Sinnott, R.K., 2013. Chemical Engineering Design: Principles, Practice, and Economics of Plant and Process Design. Butterworth-Heinemann.

Tula, A.K., Babi, D.K., Bottlaender, J., Eden, M.R., Gani, R., 2017. A computer-aided software-tool for sustainable process synthesis-intensification. Comput. Chem. Eng. 105, 74–95, http://dx.doi.org/10.1016/j.compchemeng.2017.01.001.

Valadi, J., Siarry, P., 2014. Applications of Metaheuristics in Process Engineering. Springer International Publishing, http://dx.doi.org/10.1007/978-3-319-06508-3.

Vanden Bussche, K.M., Froment, G.F., 1996. A Steady-State Kinetic Model for Methanol Synthesis and the Water Gas Shift Reaction on a Commercial Cu/ZnO/Al2O3 Catalyst. J. Catal. 161, 1–10.

Vázquez-Rowe, I., Iribarren, D., Iribarren, D., 2015. Review of life-cycle approaches coupled with data envelopment analysis: launching the CFP + DEA method for energy policy making. Sci. World J. 2015, 1–10, http://dx.doi.org/10.1155/2015/813921.

Vázquez, D., Fernández-Torres, M.J., Ruiz-Femenia, R., Jiménez, L., Caballero, J.A., 2018a. MILP method for objective reduction in multi-objective optimization. Comput. Chem. Eng. 108, 382–394, http://dx.doi.org/10.1016/j.compchemeng.2017.10.021.

Vázquez, D., Ruiz-Femenia, R., Jiménez, L., Caballero, J.A., 2018b. MILP models for objective reduction in multi-objective optimization: error measurement considerations and non-redundancy ratio. Comput. Chem. Eng. 115, 323–332, http://dx.doi.org/10.1016/J.COMPCHEMENG.2018.04.031.

Wernet, G., Bauer, C., Steubing, B., Reinhard, J., Moreno-Ruiz, E., Weidema, B.B., Zah, R., Org, W., 2016. The ecoinvent database version 3 (part I): overview and methodology. Int. J. Life Cycle Assess. 21, 1218–1230, http://dx.doi.org/10.1007/s11367-016-1087-8.

Wu, W., Yenkie, K., Maravelias, C.T., 2017. A superstructure-based framework for bio-separation network synthesis. Comput. Chem. Eng. 96, 1–17, http://dx.doi.org/10.1016/J.COMPCHEMENG.2016.10.007.

Ye, W., You, F., 2016. A computationally efficient simulation-based optimization method with region-wise surrogate modeling for stochastic inventory management of supply chains with general network structures. Comput. Chem. Eng. 87, 164–179, http://dx.doi.org/10.1016/j.compchemeng.2016.01.015.

Yue, D., Kim, M.A., You, F., 2013. Design of sustainable product systems and supply chains with life cycle optimization based on functional unit: general modeling framework mixed-integer nonlinear programming algorithms and case study on hydrocarbon biofuels. ACS Sustain. Chem. Eng. 1, 1003–1014, http://dx.doi.org/10.1021/sc400080x.

Yue, D., Pandya, S., You, F., 2016. Integrating hybrid life cycle assessment with multiobjective optimization: a modeling framework. Environ. Sci. Technol. 50, 1501–1509, http://dx.doi.org/10.1021/acs.est.5b04279.

Zhou, P., Ang, B.W., Poh, K.L., 2008a. A survey of data envelopment analysis in energy and environmental studies. Eur. J. Oper. Res. 189, 1–18, http://dx.doi.org/10.1016/j.ejor.2007.04.042.

Zhou, P., Ang, B.W., Poh, K.L., 2008b. Measuring environmental performance under different environmental DEA technologies. Energy Econ. 30, 1–14, http://dx.doi.org/10.1016/j.eneco.2006.05.001.

Zitzler, E., Thiele, L., 1998. Multiobjective optimization using evolutionary algorithms — a comparative case study. Parallel Problem Solving from Nature — PPSN V, 292–301, http://dx.doi.org/10.1007/BFb0056872.